FUNCTIONAL STUDIES ON THE N-TERMINAL REGION OF PHOTOACTIVE YELLOW PROTEIN

By

DANNY L. MAPLES

Bachelor of Arts in Chemistry
Southwestern Oklahoma State University
Weatherford, OK
2006

Submitted to the Faculty of the
Graduate College of the
Oklahoma State University
in partial fulfillment of
the requirements for
the Degree of
DOCTOR OF PHILOSOPHY
July, 2015

FUNCTIONAL STUDIES ON THE N-TERMINAL

REGION OF PHOTOACTIVE YELLOW PROTEIN

Dissertation Approved:

Dr. Wouter Hoff

Dissertation Adviser

Dr. Kevin Ausman

Dr. Nicholas Materer

Dr. Patricia Canaan

Outside Committee Member

Name: Danny Maples

Date of Degree: July, 2015

Major Field: Chemistry

Title of Study: FUNCTIONAL STUDIES ON THE N-TERMINAL REGION OF PHOTOACTIVE YELLOW PROTEIN

Abstract:

Stimulus-induced release of helical elements attached to a PAS core is a recurring feature in PAS domain protein signaling. Photoactive yellow protein (PYP) is a bacterial PAS domain photoreceptor, which contains *p*-coumaric acid (*p*CA) as its chromophore, and serves as a model system for such conformational dynamics. Deletion of the N-terminal 25-residue helical extension in PYP slows down the decay of the pB signaling state in the PYP photocycle ~1850-fold. Here we explore the mechanism by which the N-terminal region facilitates pB decay in the protein. The addition of a synthetic peptide corresponding to the N-terminal 25 residues to the Δ25 PYP mutant accelerates pB decay, but only by a factor ~4 and with poor peptide affinity (~10 mM). The strong pH-dependence of this peptide effect implies a key role for electrostatic interactions between the negatively charged N-terminal region and the positively charged PAS core, a conserved feature in the PYP family. Our results imply a critical role for the covalent tethering of the N-terminal region by increasing local concentration and by causing directional collisions that avoid non-productive associations. Unexpectedly, attachment of an N-terminal His-tag to Δ25 PYP accelerates pB decay, implying low sequence specificity for the functioning of the N-terminal region. Progressive deletion of the N-terminal extension indicates that its secondary structure only modestly affects pB decay. These results imply that the strong variation in pB decay kinetics observed in the PYP family results mainly from substitutions in the PAS core, and that non-specific but directional and electrostatically guided molecular collisions between the N-terminal extension and the PAS core control the signaling kinetics in PYP.

TABLE OF CONTENTS

LIST OF TABLES

Table Page

LIST OF FIGURES

Figure Page

CHAPTER I

INTRODUCTION

1.1 Overview

Recent developments in the life sciences include the determination of the amino acid sequences of large numbers of proteins due to great improvements in DNA sequencing technology. To help analyze such data advanced bioinformatics methods with increased sensitivity have been developed that can identify weak amino acid sequences similarities in proteins, and these have revealed that many proteins contain short (~100 residues) conserved domains, and that the shuffling of such domains is important in protein evolution[1]. These conserved domains form large protein superfamilies that share a common three-dimensional fold, but are highly diverse with respect to both their amino acid sequence and functional properties[2, 3]. Often a linker region joins these conserved domains to each other in the same protein. The overall functional properties of such proteins were often studied based on the function of each of the conserved domains. However, more recent evidence indicates that the linker regions play a significant role in protein function, and this has sparked much research interest into the mechanism of how such linkers act[4, 5].

In many instances the linker region is composed of either an N-terminal or C-terminal α-helical extension that packs tightly against a conserved β-sheet domain[6]. Conformational changes such as the stimulus-induced release and partial unfolding of the α-helical regions are thought to be functionally important in the protein[7-11]. In this thesis, the functional importance of the N-terminal helical extension of Photoactive Yellow Protein (PYP), a member of the PAS domain superfamily, is studied.

1.2 The PAS domain superfamily

Per Arnt Sim (PAS) is a term that stems from the first letter of the name of the three founding members of the domain superfamily: the *Drosophila* clock protein Period (Per), the aryl hydrocarbon receptor nuclear translocator protein (Arnt) and the *Drosophila* single-minded protein (Sim). This protein module appears to be involved in a wide range of regulatory and sensory functions in all domains of life[12], with over 50,000 proteins having been identified in the protein sequence database as containing a PAS domain, and 43 PAS domains present in the human genome[3]. PAS domains have been identified in a many signaling proteins[12, 13], including transcription factors, circadian clock proteins, phytochrome, and other proteins involved in regulation, photosensing, and oxygen/redox sensing. Interestingly, all members of this diverse set of proteins appear to be involved in sensing or regulation.

1.3 Origin of the Photoactive Yellow Protein (PYP)

In the mid-1980s Terry Meyer discovered a small water-soluble, colored protein, now known as Photoactive Yellow Protein (PYP), during the isolation and characterization of photosynthetic electron transfer proteins from the bacterium

Ectothiorhodospira halophila [14]**.** This purple bacterium was later renamed *Halorhodospira halophila*. *H. halophila* is an anaerobic, gram-positive, phototrophic organism, which can survive in extreme environmental conditions. It was originally isolated in mud taken from Summer Lake in Lake County, Oregon but has also been found in bodies of water such as the Wadi El Natrun lakes in Egypt[15, 16]. A common feature of these waters is their extreme salinity. For *H. halophila* the optimal growth range is 11-22% NaCl, but it has the ablility to survive even in 36% salt[17]. Thus, *H. halophila* has become known as an extreme halophile (salt-loving).

Being a phototropic organism, *H. halophila* requires light as its source of energy and the environments it inhabits have an abundance of sunlight. Yet, the bacterium must maintain a delicate balance between light that is used as an energy source (photosynthetic) and light such as ultraviolet radiation that can cause damaging effects. For this the bacterium has developed a mechanism called phototaxis that allows it to sense light, which it either swims toward (positive phototaxis), or swims away from (negative phototaxis). Bacteria swim by rotating flagella, and it was found that green light attracted the bacterium, but blue light induced a reversal in flagella rotation, causing the bacterium to swim away. Sprenger et al determined that the wavelength dependence of this negative phototactic response matches the absorbance spectrum of the Photoactive Yellow Protein. Therefore, PYP is thought to function as the primary photosensor in this response to blue light[18].

1.4 General properties of PYP

PYP is a small water-soluble globular protein containing 125 amino acids (Figure 1.1) with a molecular weight of 14 kDa[19]. It is highly thermostable (T_m ~85 °C), and has an intense bright yellow color due to the presence of a small chromophore, which absorbs blue light at a maximum wavelength of 446 nm (Figure 1.2).

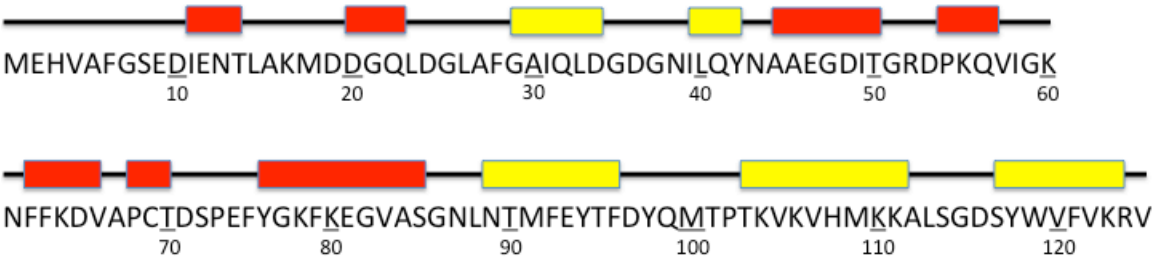

Figure 1.1: The PYP amino acid sequence. Secondary structures are shown above the amino acid sequence. Alpha helices are shown in red and β-sheets are shown in yellow.

Initially, it was thought that the PYP chromophore was a retinal molecule bound to a lysine residue in the protein through an Schiff base[20], similar to the chromophore properties of the sensory rhodopsins. However, this was proven not to be the case when Van Beeumen et al. showed that PYP contained a chromophore with a molecular weight of ~147 Daltons, which was covalently bound to the unique cysteine residue (Cys69) in PYP[19]. Further chemical analysis by two independent research groups confirmed that the chromophore is 4-hydroxy cinnamic acid (also termed *p*-coumaric acid or *p*CA), and is covalently bound to the sulfur side-chain of Cys69 via thio-ester bond (Figure 1.3)[21, 22].

Thus, PYP is the first protein to have been determined to contain the *p*CA chromophore. Other proteins from different bacterial species have been found to contain this chromophore, similar to PYP. These have been grouped into a family of blue light photoreceptors that contain *p*CA called the Xanthopsins[23].

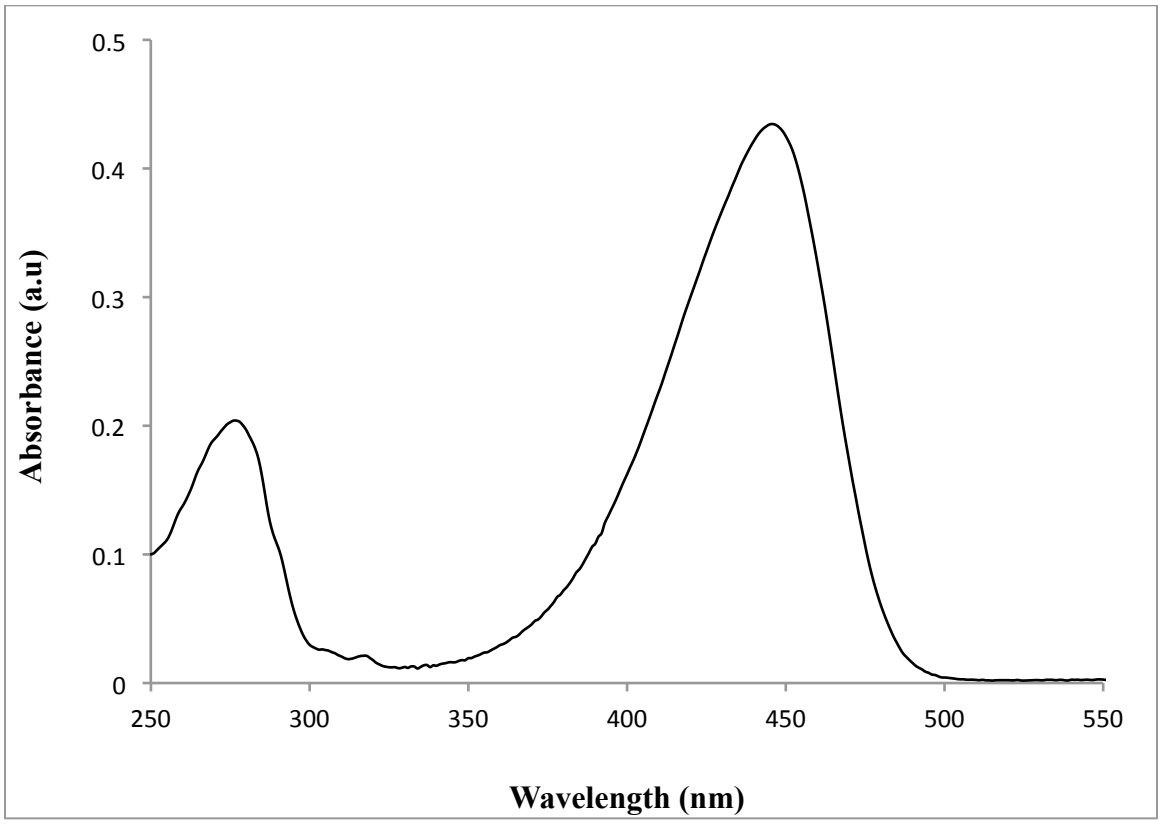

Figure 1.2: **The PYP absorbance spectrum.** The absorbance spectrum of wild-type PYP in 10 mM Tris, pH 7.4. The absorbance maximum for ground state *p*CA is at 446 nm.

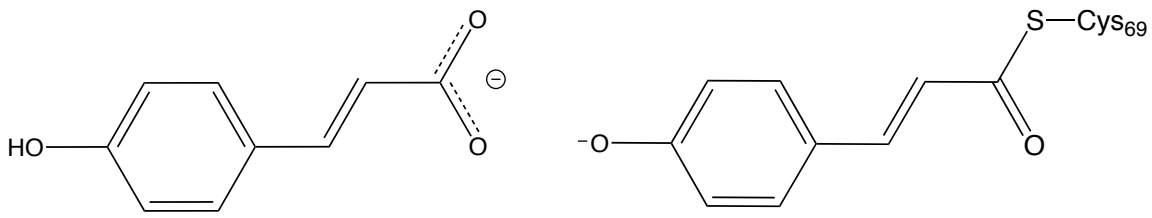

Figure 1.3: **Structure of *p*CA.** (A) Structure of *p*CA in solution at neutral pH. (B) Structure of ground state *p*CA bound to cysteine-69 in PYP.

The biophysical and biochemical properties of PYP have been extensively studied due to several attractive features of the protein. It contains the *p*CA chromophore, which exhibits a light-triggered photocycle. PYP is easily handled; it can be over-expressed in *E. coli*, and has both high solubility and excellent thermostability.

1.5 Structure of PYP: a PAS domain prototype

High-resolution 3D-structures for PYP are now available from X-ray diffraction[24,25] and Nuclear Magnetic Resonance (NMR) studies[18, 26] and have been deposited in the Protein Data Bank (PDB). These have shown that PYP is globular and adopts a α/β folded tertiary structure (Figure 1.4) that essentially forms two distinct regions in the protein: the N-terminus (residues 1-28) and the PAS core (residues 29-125). In literature, the structure is further described as four distinct regions: 1) the N-terminal cap (residues 1-28), 2) the PAS core (residues 29-69), comprising the first three β-strands, 3) an α-helical connector (residues 70-87), and 4) the β-scaffold (residues 88-125), comprising the last three β-strands[27]. The PAS domain is composed of a six-

stranded anti-parallel β-sheet surrounded by three α-helices, which is folded into a clam-like structure, forming a large hydrophobic cavity. The *p*CA chromophore resides inside this hydrophobic cavity covalently bound via thio-ester bond to cysteine-69. In the ground state configuration (pG) of PYP the *p*CA chromophore is deprotonated and negatively charged on the phenolic oxygen. This buried charge inside the protein is stabilized by hydrogen bonding interactions between nearby residues Glu46 and Tyr 42, as well as interaction between the C=O group of *p*CA and the NH backbone of Cys69. On the opposite side of the β-sheet (opposite to the chromophore) lies the N-terminus region, composed of two small α-helices that cap the backside of the β-sheet, creating a smaller hydrophobic core.

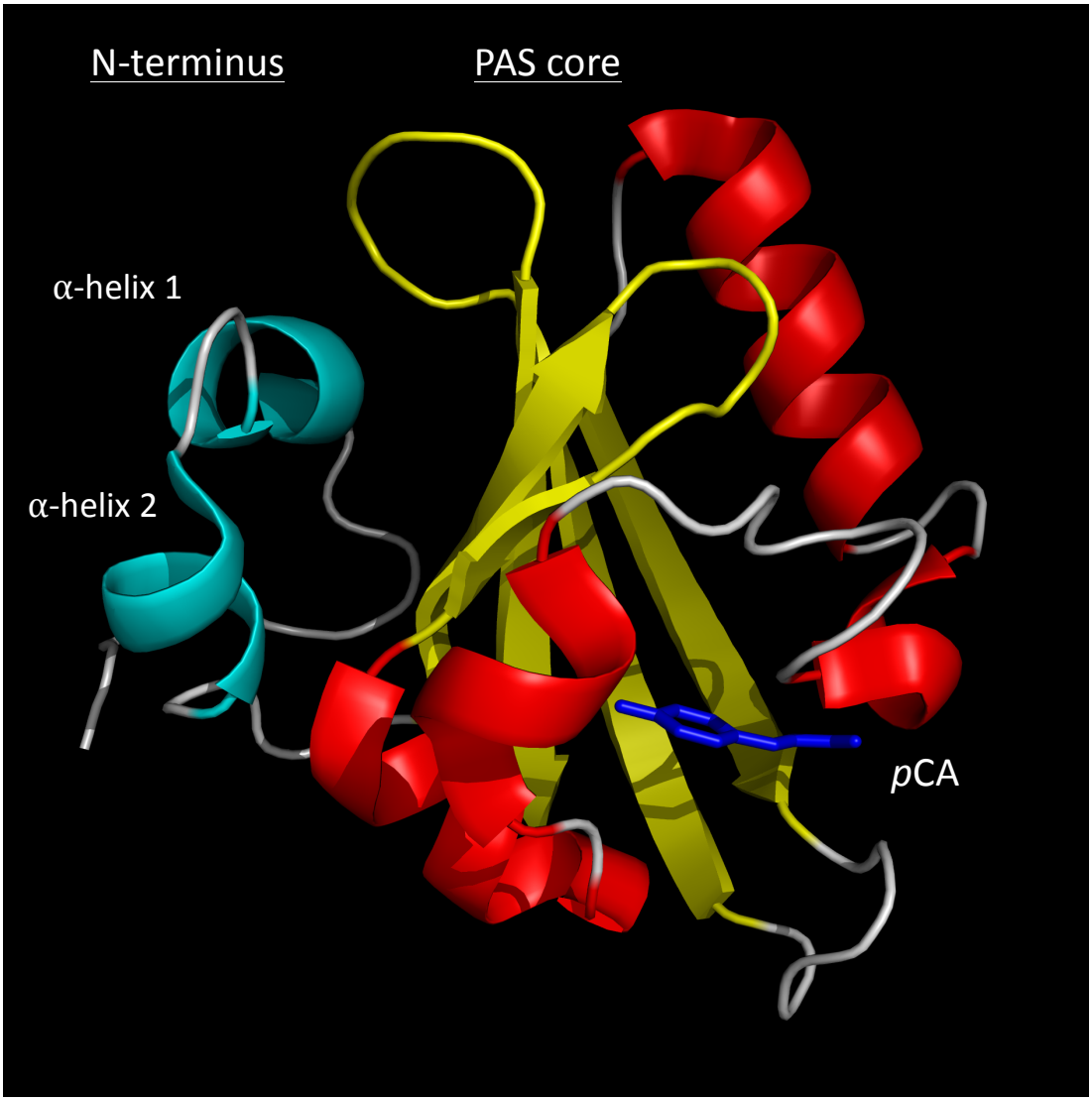

Figure 1.4: The PYP PAS domain structure. Crystal structure of wild type PYP (1NWZ) from *Halorhodospira halophila* showing the location of the N-terminal region (in light blue) containing two α-helices in relation to the *p*CA chromophore (blue) and PAS core (with α-helices in red and β-strands in yellow).

1.6 PYP photocycle

The photocycle and kinetics of PYP show some similarity to the sensory rhodopsins from halobacteria, and to bacteriorhodopsin and halorhodopsin[28]. In PYP, the photocycle (Figure 1.5) is initiated by ground state (pG) absorption of blue light (λ_{max} = 446 nm) (ε = 45 500 $M^{-1}cm^{-1}$) by the *p*CA chromophore. In pG the *p*CA is in the trans conformation and the phenolic oxygen is deprotonated, while the carboxyl group of Glu46 is protonated. This buried charge is stabilized through hydrogen-bonding networks between Glu46 and Tyr42, Thr50 and Tyr42, and between the C=O of *p*CA and the NH backbone of Cys69. Additionally, the buried negative charge may be stabilized by the positive charge of the neighboring Arg52 side chain. Upon blue photon absorption the *p*CA undergoes trans-cis isomerization, leading to a red-shifted intermediate (pR) (λ_{max} = 465 nm) in which the phenolic oxygen of the chromophore remains deprotonated[29]. In a few hundred microseconds this intermediate decays to a blue-shifted intermediate (pB') (λ_{max} = 355 nm) in which the *p*CA phenolic oxygen has become protonated via intramolecular proton shift from nearby Glu46. This eliminates the negative charge from the chromophore and creates a new charge buried negative charge on Glu46. In about 2 ms this charge transfer event induces a global rearrangement in the protein structure to occur resulting in the long-lived, blue-shifted pB intermediate, which is characterized by the partial unfolding and stimulus-induced release of the N-terminal region from the PAS core. This long-lived pB intermediate is presumed to be the signaling state of PYP that effects downstream cell motility. To complete the photocycle the pB intermediate must decay back to pG ground state. This occurs on the sub-second time scale and involves the refolding of PYP to its native state, cis-trans reisomerization of *p*CA, and proton transfer

from the phenolic oxygen back to Glu46. In this work we are only concerned with this transition; the decay of the pB intermediate back to the pG ground state.

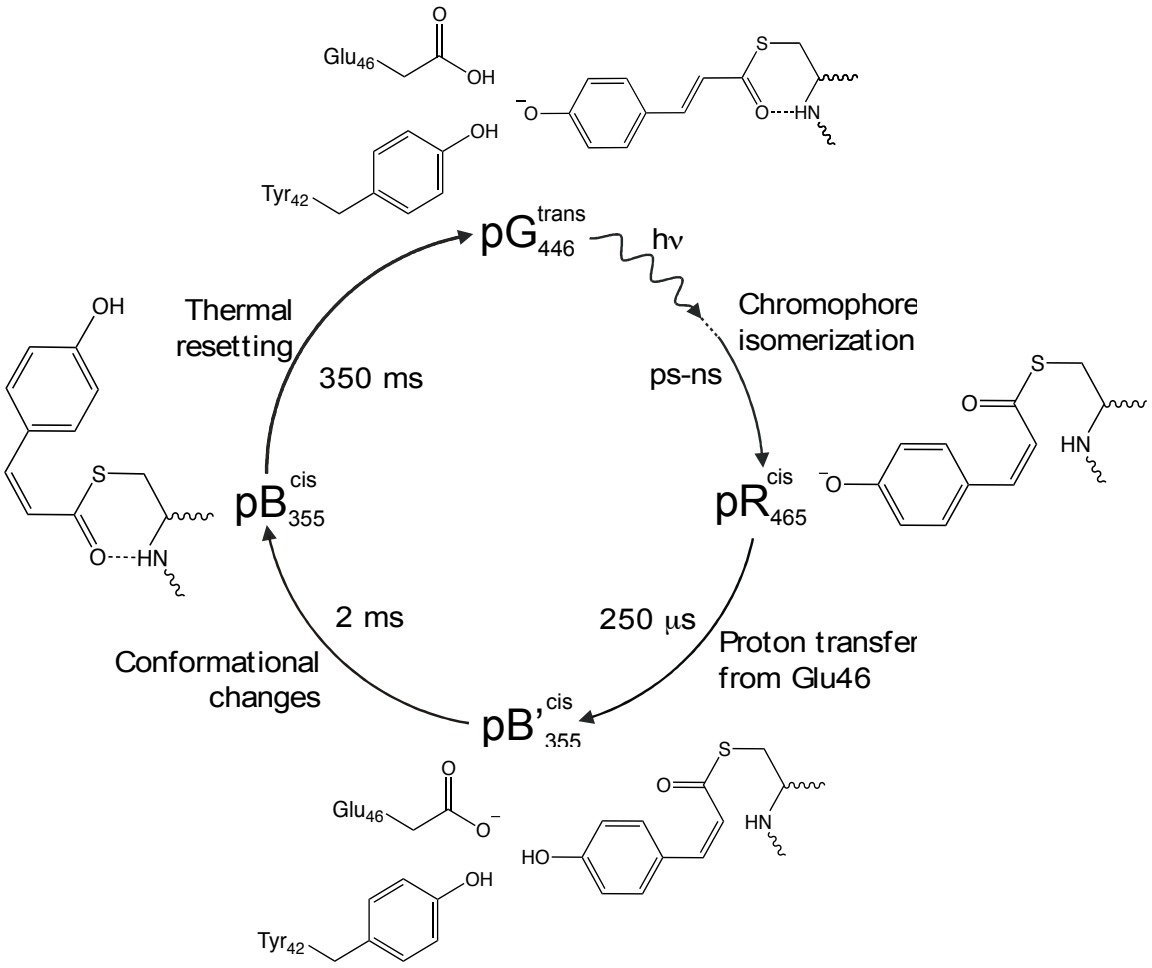

Figure 1.5: **The PYP photocycle based on UV-visible absorbance spectroscopy.** The pG ground state and major intermediates of the PYP photocycle are shown, along with the conformational changes of the *p*CA chromophore. The subscripts denote the absorbance maximum of each state and the superscripts denote the isomerization state of *p*CA.

1.7 N-terminal deletions in PYP affect the pB decay rate

An emerging theme from various studies of PAS domains is the functional importance of N-terminal or C-terminal α-helical extensions. Many of these helical extensions pack against the β-sheet of the PAS core similar to the N-terminus of PYP. Examples of these include the N-terminal α-helical extension of the fungal photoreceptor Vivid[11], the C-terminal extension of the *Drosophila* clock protein Period[10], and the Jα helix, a C-terminal helical extension from the LOV-based plant phototropin[9]. Stimulus-induced release and partial unfolding of these helical extensions have been reported, and are thought to be functionally important[7-11]. For many of these, the helical extension serves as a linker from the PAS domain to another regulatory domain in the same protein, and it is thought that conformational changes in the linker region results in signal relay from one domain to another. However, it is not clear how this occurs.

In PYP, the N-terminal region contains two small α-helices that fold against the central β-sheet of the PAS core (Figure 1.4). These are made of residues 11-14 (α1) and residues 19-22 (α2) according to the PYP crystal structure 1NWZ. In the long-lived photocycle intermediate pB this N-terminal region is reported to partially unfold and is released from the central β-sheet of the PAS core[30-35]. This is thought to be the signaling state of PYP. Partial or complete deletion of the N-terminal region causes a major reduction in the pB decay rate. Yet, while several N-terminally truncated variants of PYP have been reported[30, 36-39], the mechanism by which the N-terminus accelerates the pB decay rate in the photocycle of PYP remains mostly unknown.

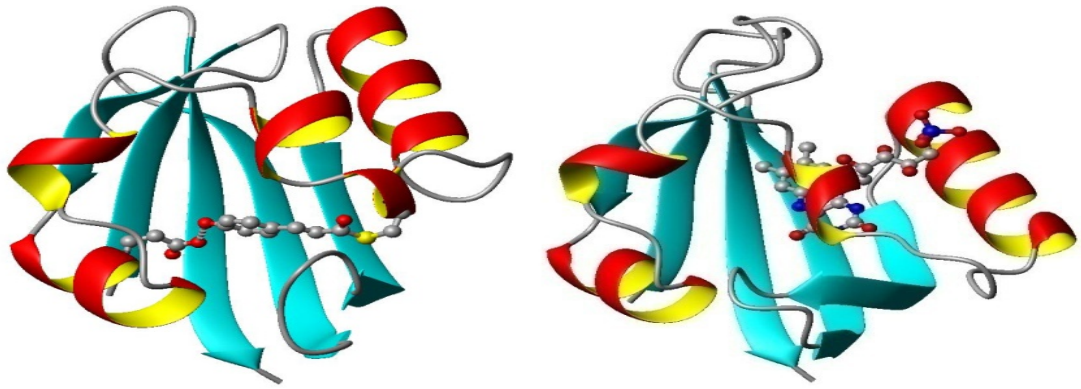

Figure 1.6 Other PAS domain proteins. The structures of Δ25 PYP with *p*CA chromophore and LOV2 with flavin mononucleotide (FMN) chromophore.

1.8 Aims of this research

In this study, the N-terminal deletion mutant Δ25 PYP (Figure 1.6) from *H. halophila* was used to gain insight into the mechanism of how the N-terminal α-helical extension accelerates the decay rate of the last-step pB signaling intermediate in PYP. To accomplish this we first synthesized and purified Δ25 PYP lacking the amino acid residues 1-25. A synthesized 25-mer peptide corresponding to residues 1-25 of the N-terminal region of PYP was added to purified Δ25 PYP at various peptide concentrations in order to accelerate pB decay. Next, since the N-terminal peptide was not tethered (covalently bound) to Δ25 PYP and it was thought that the peptide was most likely

unstructured (not folded or having α-helical structure), we used various additives in order to induce structure in the peptide and increase non-covalent interactions between the N-terminal peptide and Δ25 PYP. To further understand which residues in the N-terminus of PYP affect the pB decay rate we made a series of PYP deletion mutants in which the residues of the N-terminus were consecutively deleted and their pB decay rates were compared.

In all of these experiments transient UV-visible absorbance spectroscopy was used to monitor the pB decay kinetics of Δ25PYP and all deletion mutants. Samples were photo-bleached with blue light until steady-state pB formation, then pB decay kinetics was monitored in the dark until completion of the PYP photocycle.

CHAPTER II

Experimental Procedures

2.1 Overview of Chapter 2

This chapter covers the cloning, expression, and purification of Δ25 PYP as well as the PYP deletion mutants that were made. Spectral and kinetic analysis will also be discussed. The design of the initial experiment was to overexpress Δ25 PYP and purchase the 25-mer peptide that corresponds to the N-terminal amino acid residues 1-25 of full-length PYP. Δ25 PYP along with various concentrations of peptide would be mixed together and placed into a cuvette in the UV/Vis spectrometer. The sample would be covered and allowed to remain in the dark for 10 minutes to ensure the sample was in the pG ground state and not bleached by the room light. Then, the sample would be bleached with blue light, by using a fiber optic light source with a broad band blue filter, until steady state pB formation had occurred, and the rate (absorbance as a function of time) of pB decay (pG recovery) would be monitored in the dark at the absorbance maximum (442 nm) of Δ25 PYP. We hypothesized that the addition of the N-terminal peptide to Δ25 PYP would recover the same pB decay rate as full-length PYP

(~0.5 s) at some concentration of synthetic N-terminal peptide. However, this was not the case and therefore other experiments were undertaken in order to determine why, and if the recovery rate could be increased, for example, by the addition of salts or structure inducing agents, by pH titration, etc. In order to get a better understanding of how the N-terminal region speeds up the pB decay rate and which amino acid residues may contribute to this increase, a series of deletion mutants were made in which residues were consecutively deleted from the N-terminus and the pB decay rate was determined for each of these.

2.2 Cloning, expression, and purification of Δ25 PYP

2.2.1 Initial cloning into pET-26b

Initially, Δ25 PYP was cloned into a pET-26b vector. This vector does not encode an affinity tag to aid in purification, but we planned to purify the protein by anion exchange chromatography. However, this was not the case as Δ25 PYP would not bind to the anion exchange column, even in the dark state. Since Δ25 PYP without affinity tag could not be easily purified it was cloned into a pET-46 Ek/LIC vector which encoded a hexa-histidine affinity tag (MAHHHHHHVDDDK) on the N-terminal end of the protein. This histidine tag allowed for the purification of Δ25 PYP by both metal affinity and anion exchange chromatography. Upon purification the histidine tag was removed from Δ25 PYP by the enzyme enterokinase.

2.2.2 Cloning Δ25 PYP into pET-46 Ek/LIC

The forward and reverse primers used for cloning Δ25 PYP into the pET-46 Ek/LIC vector (Novagen), (Figure 2.1) were purchased from Invitrogen. The forward

primer (5' **GAC GAC GAC AAG** ATG GCC TTC GGC GCC 3') includes nucleotides necessary for insertion into the Ligation Independent Cloning (LIC) vector (bolded), and nucleotides to encode the first five amino acids of Δ25 PYP. The reverse primer (5' **GAG GAG AAG CCC GGT** CTA GAC GCG CTT GAC GAA GAC 3') includes the complementary nucleotides necessary for the overhang regions of the LIC vector (bolded), as well as those encoding the last six amino acids of PYP, and a STOP codon.

The Polymerase Chain Reaction (PCR) using the forward and reverse primers, along with full-length PYP in pQE-80L plasmid as a template, was used to create the gene for Δ25 PYP. The PCR product was electrophoresed on a 2% agarose gel to check that the DNA insert of correct size (~400 bp) was formed. After confirmation, the PCR product was electrophoresed on a 2% low-melting agarose gel and the DNA band of appropriate size was excised and then purified using a Qiagen QIAquick Gel Extraction Kit.

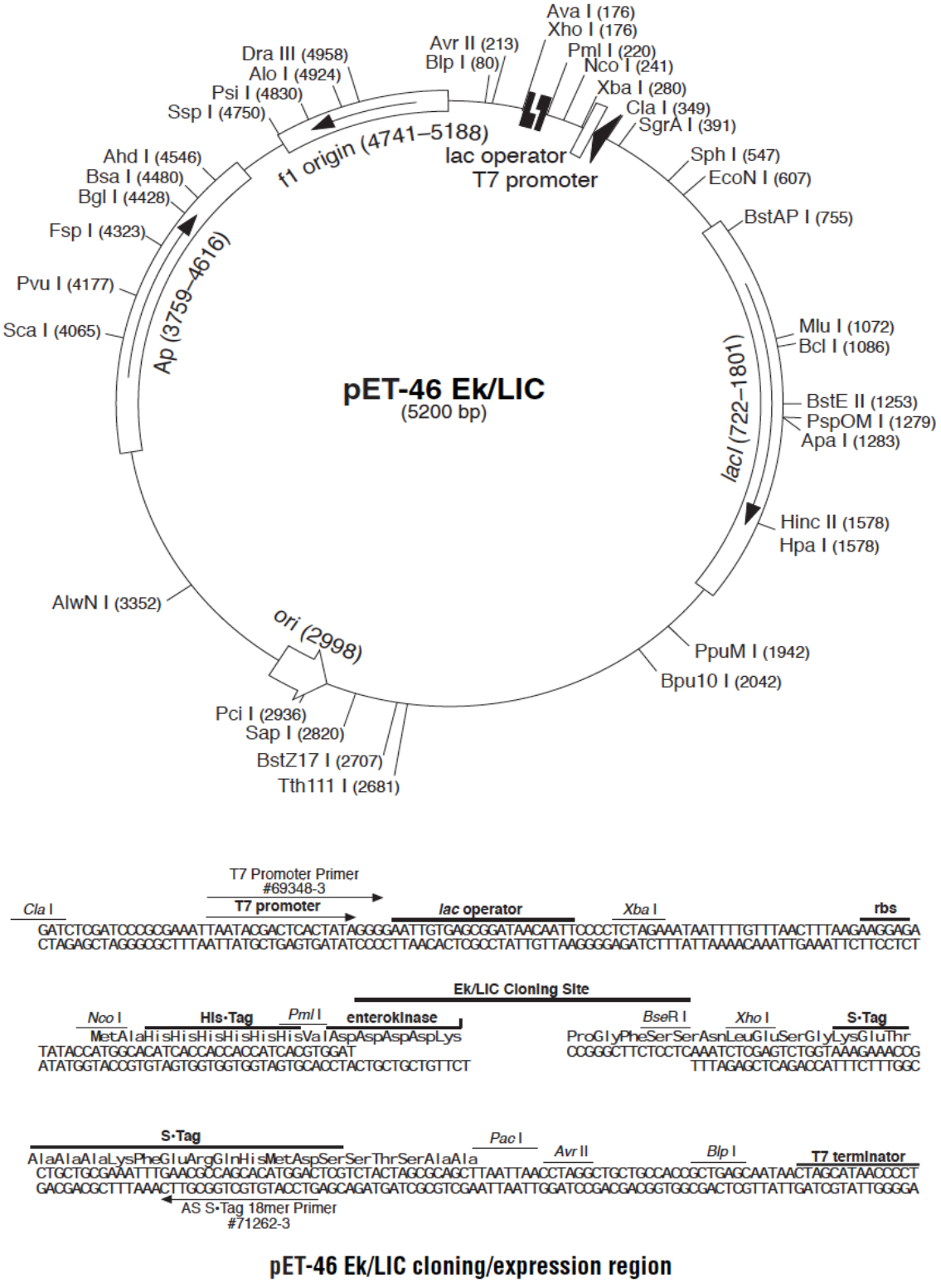

Figure 2.1: The pET-46 Ek/LIC vector map. A map of the pET-46 Ek/LIC vector used for cloning and expression of Δ25 PYP and the PYP deletion mutants.

After extraction and purification from the agarose gel, the Δ25 PYP DNA insert was then treated with T4 DNA Polymerase to create complimentary DNA extensions to each end in order to anneal to the linearized pET 46-EK/LIC vector. The 20 μL reaction mixture for T4 DNA Polymerase treatment consisted of 10 μL of gel-purified DNA insert, 2.5 mM dATP, 5 mM DTT, 1 Unit of T4 DNA Polymerase, 1x DNA polymerase buffer, and 4.6 μL of nuclease-free water. The mixture was incubated at room temperature for 40 minutes and then the T4 polymerase enzyme was inactivated in a 75°C water bath for 20 minutes, according to the manufacturer's protocol. After T4 DNA Polymerase treatment of the Δ25 PYP insert the vector and insert were annealed together creating a plasmid that could be transformed into bacteria. This reaction mixture consisted of 3 μL of the T4 DNA Polymerase treated Δ25 PYP insert along with 1 μL of linearized pET-46 Ek/LIC vector. This mixture was incubated for 5 minutes at room temperature and then 1 μL of 25 mM EDTA was added per manufacturer protocol. As a negative control for this reaction nuclease-free water was used in place of the Δ25 PYP DNA.

2.2.3 Plasmid transformation into E. coli GigaSingles

Transformation into bacteria was accomplished by adding all 5 μL of the plasmid DNA to 50 μL of chemically competent *E. coli* cells (GigaSingles, Novagen). These bacteria are used for storage and maintenance of the plasmid, not for the expression of protein. The reaction mixture was incubated on ice 5 minutes then heat-shocked in a 42°C water bath for 1 minute, and put back on ice for 2 minutes. This step causes the plasmid to be taken up by the bacteria. Next, 250 μL of SOC medium was added to the bacteria cells and the mixture was incubated for 1 hour at 37°C. After the one hour

incubation period 50 μL of the mixture was plated on Luria-Burtani (LB) agar plates containing 50 μg/mL ampicillin and left to incubate overnight at 37 °C. The same procedure was repeated for the negative control. After the overnight incubation the negative control agar plate had about 20 bacterial colonies and the insert agar plate had about 300 bacterial colonies. Bacterial colony PCR and subsequent agarose gel electrophoresis showed a band for the 300 bp Δ25 PYP insert. LB medium containing 50 μg/mL ampicillin was inoculated with a single colony and incubated overnight at 37°C and 200 rpm shaking. A portion of the overnight culture was used to make glycerol stocks and these were stored at -80°C. The Δ25 PYP-pET-46 Ek/LIC plasmid was extracted and purified from the remainder of the bacteria cells using a Qiagen QIAprep Spin Miniprep Kit. The resulting DNA sample was sent to the OSU DNA sequencing facility, which confirmed the Δ25 PYP insert was in the correct orientation, along with the N-terminal hexa-histidine tag and the enterokinase (Ek) cleavage site.

2.2.4 Plasmid transformation into E. coli BL21 (DE3)

After confirmation that the sequence was correct the plasmid was transformed into a bacterial expression strain in order to produce the Δ25 PYP protein. For this reaction 2 μL of plasmid DNA was mixed with 20 μL of BL21 (DE3) competent bacterial cells and incubated on ice 5 minutes. Then the cells were heat-shocked at 42°C for 45 seconds in a water bath and put back on ice 2 minutes. Next, 80 μL of SOC medium was added to the mixture and incubated at 37°C for 3 hours. After this 50 μL of the mixture was plated onto a LB agar plate containing 50 μg/mL ampicillin and incubated overnight at 37°C. The same procedure was repeated for a negative control. After overnight incubation the negative control did not have any bacterial colonies, while the plate with

the Δ25 PYP plasmid had about 500 bacterial colonies. Two colonies were picked and grown overnight in LB medium with antibiotic. From these glycerol stocks were made and stored at -80°C and a portion was used to inoculate a larger volume of medium for a larger culture.

2.2.5 Expression of Δ25 apo-PYP

For large culture Δ25 PYP expression 2 L of autoclaved LB medium containing 50 μg/mL ampicillin in a 4 L Erlenmeyer flask was inoculated and allowed to grow overnight (~16 hours) at 37°C and 200 rpm shaking. Protein expression was induced by adding 1 mM IPTG and culture was incubated at 37°C for an additional 3-4 hours. The bacterial cells were harvested by centrifugation and the supernatant was removed. About 200 mL of 8 M urea was added to the pelleted cells and stirred to lyse the bacteria, releasing Δ25 PYP protein into the supernatant. High-speed centrifugation (25000 rpm, 20 min.) was used to clarify the supernatant containing the protein. Addition of equal volume 10 mM Tris buffer, pH 7.5 was used to dilute the urea to 4 M urea, allowing the protein to partially refold.

2.2.6 Synthesis of para Coumaric Acid (pCA) anhydride

The *p*CA anhydride was synthesized with slight modification to Immamoto, 1995 (Figure 2.2). Briefly, a 2:1 molar ratio of *trans p*-coumaric acid to dicyclohexalcarbodiimide (DCC) was added to 1 mL of N, N' dimethylformamide (DMF) and the reaction was warmed in a water bath for 10 minutes to create *trans p*-coumaric anhydride. The reaction mixture was cooled for 15 minutes at -20°C to precipitate any side products, then centrifuged, and the precipitate removed. Next, the

yellow *trans p*-coumaric anhydride was added to partially folded Δ25 PYP (containing 4 M urea) and the mixture was stirred in the dark at 4°C to allow the *p*CA to react with the thiol side-chain of the cysteine in PYP.

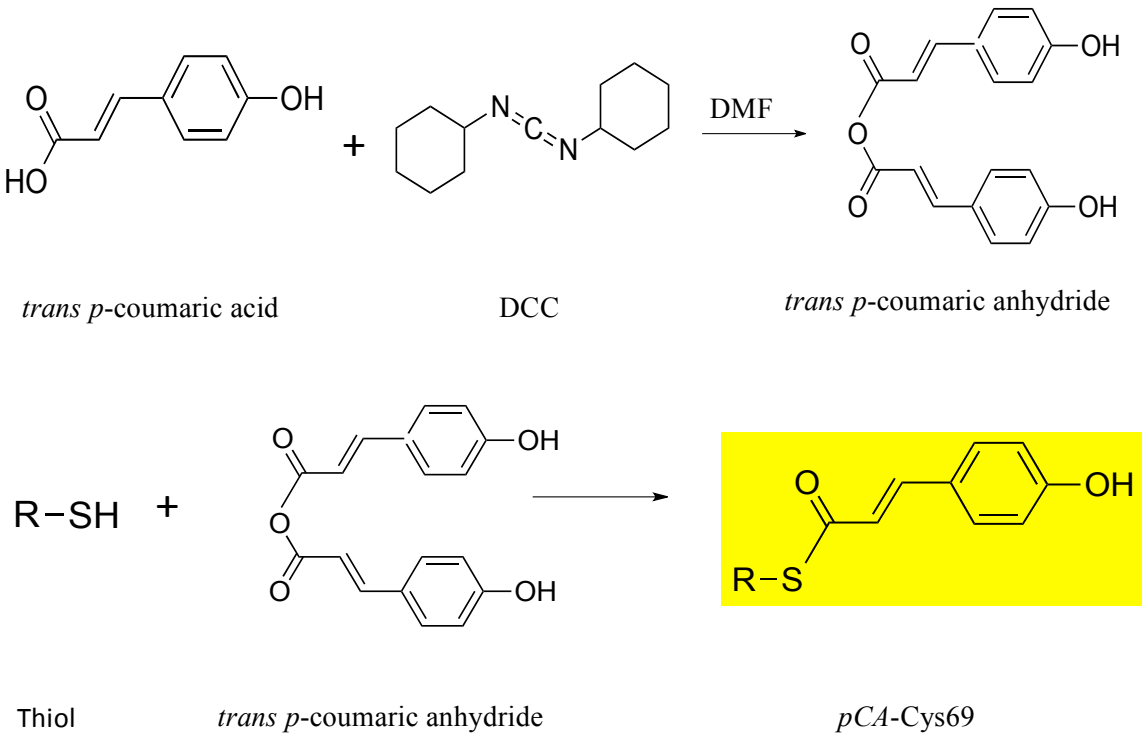

Figure 2.2: Synthesis of the *p*CA anhydride. Synthesis of the *p*CA anhydride (top panel) and subsequent reaction with the thiol side-chain of cysteine-69 in PYP (bottom panel).

2.2.7 Addition of pCA anhydride to generate Δ25 holo-PYP

At this point the *p*CA anhydride was added to the supernatant containing Δ25 PYP holo-protein and stirred for 1 hour. This allowed the *p*CA chromophore to covalently attach to the sulfur side chain of cysteine 69 via thioester formation and the supernatant turned a bright yellow color. The protein was then dialyzed against 4 L of 10

mM Tris buffer (pH 7.5) overnight using 6-8 kDa MWCO dialysis tubing. This step removed the remaining urea and small molecular weight impurities, allowing Δ25 PYP to refold.

2.2.8 Purification of Δ25 PYP

Δ25 PYP with histidine tag was much more stable than Δ25 PYP without the tag and was not appreciably bleached under ambient light. Δ25 PYP with histidine tag will selectively bind to a column containing Ni^{2+} ion. Therefore, with a histidine tag the protein can be easily purified using a combination of immobilized metal affinity chromatography (IMAC) and ion exchange chromatography (IEC). If needed, the sample can then be further purified by size-exclusion chromatography. These are standard purification techniques that are routinely utilized for aqueous proteins. Ni-NTA (MCLAB) was used for the IMAC column and DEAE-Sepharose was used for the anion exchange column. These columns can be regenerated and reused many times. Since the protein is bright yellow it is easily detected by visual inspection of the column, and visible spectroscopy can be used to check the purity of protein fractions eluted from the column. After dialysis of the protein, crude Δ25 PYP with histidine tag was loaded onto the Ni-NTA column, washed with 10 mM Tris buffer (pH 7.5), and then eluted with 200 mM imidazole. Then the eluted PYP fraction was loaded directly onto the anion exchange column, washed with low NaCl (5-15 mM) concentration to remove non-specifically bound contaminants, and then eluted with 100 mM NaCl. The absorbance at 444 nm was monitored to ensure that no Δ25 PYP was being lost. These two procedures were repeated until pure fractions were collected. Then the protein was dialyzed to

remove NaCl and imidazole. The best purity index (A_{277nm}/A_{444nm}) for Δ25 PYP with His-affinity-tag was 0.46.

2.2.9 Histidine tag removal using enterokinase

The enzyme enterokinase selectively cleaves the carboxyl end of the amino acid sequence DDDK with greater than 95% efficiency after 16 hours at 22°C. This allows the hexa-histidine tag to be easily removed from Δ25 PYP. The protein can then be loaded onto a nickel column allowing capture and removal of the cleaved tag and any remaining Δ25 with tag still attached. Δ25 without histidine tag will simply flow through the column and can be collected. After the tag is removed the small amount of enterokinase can be removed to keep the sample as pure as possible. However, anion exchange could not be used, as Δ25 without tag would not bind to the column even in the dark state. Size exclusion chromatography (gel filtration) was used to remove the remaining enterokinase and the purity was assessed by SDS-PAGE as well as visible spectroscopy. The final purity index for Δ25 without tag was 0.50-0.55 using the absorption maxima A_{277nm}/A_{442nm}.

2.3 PYP deletion mutant synthesis

The forward primers and reverse primer for the deletion mutants were purchased from Invitrogen and are listed in Table 2.1. Cloning into the pET-46 Ek/LIC vector and protein expression for the deletion mutants was performed the same as for Δ25 PYP above. However, because of the number of mutants, protein expression and purification was done in smaller amounts. Purification was done using Ni-NTA in 1.5 mL tubes to bind the histidine affinity tag on each PYP deletion mutant. About 0.5 mL of Ni-NTA

was added to a 1.5 mL tube and equilibrated by washing several times with Tris-Cl buffer, pH 7.4. Each PYP deletion mutant was added to a tube and mixed with the Ni-NTA to allow binding of the tag. The sample was then centrifuged to pellet the Ni-NTA with bound PYP and the supernatant was removed. Tris buffer was added and the sample was mixed, then centrifuged again to pellet, and the clarified supernatant removed. This was repeated 3 times in order to wash the bound PYP deletion mutant. Finally, imidazole was added to the tube and mixed in order to elute the deletion mutant. The sample was again centrifuged to pellet the Ni-NTA leaving the yellow PYP deletion mutant in the supernatant. In order to remove the histidine affinity tag the deletion mutant was incubated with enterokinase and then the sample was again added to the Ni-NTA, and mixed. This allowed for binding of the cleaved histidine affinity tag and any deletion mutant that did not have the affinity tag removed, leaving the PYP deletion mutant in which the tag was removed in the supernatant.

Deletion Mutant	**Primer Sequence**
Δ1 (E2M)	5'-**GAC GAC GAC AAG ATG** CAC GTA GCC TTC-3'
Δ2 (H3M)	5' **GAC GAC GAC AAG ATG** GTA GCC TTC GGT 3'
Δ3 (V4M)	5' **GAC GAC GAC AAG ATG** GCC TTC GGT AGC 3'
Δ4 (A5M)	5' **GAC GAC GAC AAG ATG** TTC GGT AGC GAG 3'
Δ5 (F6M)	5' **GAC GAC GAC AAG ATG** GGT AGC GAG GAC 3'
Δ6 (G7M)	5' **GAC GAC GAC AAG ATG** AGC GAG GAC ATC 3'
Δ7 (S8M)	5' **GAC GAC GAC AAG ATG** GAG GAC ATC GAG 3'
Δ8 (E9M)	5' **GAC GAC GAC AAG ATG** GAC ATC GAG AAC 3'

Δ9 (D10M)	5’ **GAC GAC GAC AAG ATG** ATC GAG AAC ACC 3’
Δ10 (I11M)	5’ **GAC GAC GAC AAG ATG** GAG AAC ACC CTC 3’
Δ11 (E12M)	5’ **GAC GAC GAC AAG ATG** AAC ACC CTC GCC 3’
Δ12 (N13M)	5’ **GAC GAC GAC AAG ATG** ACC CTC GCC AAG 3’
Δ13 (T14M)	5’ **GAC GAC GAC AAG ATG** CTC GCC AAG ATG 3’
Δ14 (L15M)	5’ **GAC GAC GAC AAG ATG** GCC AAG ATG GAC 3’
Δ15 (A16M)	5’ **GAC GAC GAC AAG ATG** AAG ATG GAC GAC 3’
Δ16 (K17M)	5’ **GAC GAC GAC AAG ATG** ATG GAC GAC GGC 3’
Δ17 (M18)	5’ **GAC GAC GAC AAG ATG** GAC GAC GGC CAG 3’
Δ18 (D19M)	5’ **GAC GAC GAC AAG ATG** GAC GGC CAG CTC 3’
Δ19 (D20M)	5’ **GAC GAC GAC AAG ATG** GGC CAG CTC GAC 3’
Δ20 (G21M)	5’ **GAC GAC GAC AAG ATG** CAG CTC GAC GGC 3’
Δ21 (Q22M)	5’ **GAC GAC GAC AAG ATG** CTC GAC GGC CTG 3’
Δ22 (L23M)	5’ **GAC GAC GAC AAG ATG** GAC GGC CTG GCC TTC 3’
Δ23 (D24M)	5’ **GAC GAC GAC AAG ATG** GGC CTG GCC TTC 3’
Δ25 (L26M)	5’ **GAC GAC GAC AAG ATG** GCC TTC GGC GCC ATC3’
Δ26 (A27M)	5’ **GAC GAC GAC AAG ATG** TTC GGC GCC ATC 3’
Δ27 (F28M)	5’ **GAC GAC GAC AAG ATG** GGC GCC ATC CAG 3’
Reverse primer	5’ **GAG GAG AAG CCC GGT** CTA GAC GCG CTT GAC GAA GAC 3’

Table 2.1: PYP deletion mutant primers. PYP deletion mutants with corresponding forward primers and the reverse primer used for insertion into pET-46 Ek/LIC vector. Nucleotides necessary for annealing into the vector are bolded.

2.4 Absorbance spectroscopy

2.4.1 Overview

All absorbance data were measured using either a Hewlett-Packard HP-8453 diode array UV-Visible spectrophotometer or a Synergy HT Multi-Detection Microplate Reader (Bio-Tek Instruments). A 150 W halogen quartz light source (Cuda) with optical fiber light guide and a broadband blue filter (band-pass filter 59855, Oriel) was used to initiate the PYP photocycle. All experiments were performed in dark conditions at room temperature. Typically, 10 μM Δ25 PYP samples in 50 mM MOPS (pH 7.5), with or without 25-mer peptide, salts, or other additives were placed in a 10 mm path length quartz cuvette (and in some cases a 1 mm path length cuvette) and illuminated with blue light until steady-state pB formation was reached. The microplate reader was used to simultaneously measure multiple samples with slow pB decay kinetics in a 96-well plate. The plate was placed into the instrument plate holder and the wells were illuminated with blue light for about 2 minutes for steady state photo bleaching of the PYP samples. The plate reader door was immediately closed and absorbance measurements at 442 nm were initiated and continued until completion of the photocycle. Absorption spectra at 442 nm as a function of time were collected in the dark to monitor pB decay.

2.4.2 General data analysis

All absorption data were analyzed in IGOR Pro version 6.2 (Wave Metrics, Inc) to obtain pB decay rates. Time-resolved light-induced difference spectra of PYP samples were determined by subtracting the dark state absorbance spectra from the photobleached spectra. For the samples analyzed here the process of pB decay was found to be

monoexponential except when stated otherwise. In this thesis, the peptide effect on pB decay rate is the ratio of rates of pB decay in the absence and presence of N-terminal peptide, and the salt or additive effect is the ratio of rates in the absence and presence of the respective salt or additive.

2.4.3 Purchase and reconstitution of the N-terminal peptide

The synthetic 25-mer peptide MEHVAFGSEDIENTLAKMDDGQLDG-amide (100 mg), corresponding to the N-terminus of full length PYP, was purchased from Genemed Synthesis Inc. (San Antonio, TX), and was received as a white lyophilized powder. Peptide purity was >95% with an average mass 2722.4 amu. The peptide was dissolved in 50 mM MOPS, pH 9 and subsequently adjusted to pH 7.5 using NaOH, to yield a 50 mg/mL concentration. This stock peptide solution was used in all peptide experiments.

2.4.4 Circular dichroism (CD) spectroscopy of the N-terminal peptide

The CD spectrum of the free N-terminal peptide was taken in order to determine whether its secondary structure contained α-helical content similar to the full-length PYP N-terminus determined by NMR spectroscopy and crystallography. CD spectra from 190-260 nm for two different 0.2 mg/mL 25-mer peptide solutions in 20 mM sodium phosphate (pH 7.3) were obtained using a JASCO J815 spectrometer. Analysis of the CD spectra to estimate secondary structure content was performed using two different online servers: K2D3 (http://k2d3.ogic.ca/) and AGADIR (http://agadir.crg.es/). K2D3 uses a database of theoretically derived CD spectra to calculate the percent α-helical and β-sheet content from a protein's CD spectrum. AGADIR is a prediction algorithm based on the

helix/coil transition theory that is used to predict the helical behavior of small monomeric peptides.

2.4.5 Addition of N-terminal peptide to Δ25 PYP

To measure the effect of the N-terminal peptide on pB decay in Δ25 PYP, 10 μM Δ25 PYP and the peptide, both in 50 mM MOPS buffer at pH 7.5, were mixed together to give a 0-15 mM final peptide concentration. All samples (200 μL) were placed into a 96-well plate, bleached with blue light until steady state pB formation, and pB decay kinetics was monitored at 442 nm in the dark. The resulting kinetic traces were analyzed to obtain pB decay rates and these rates were fit using our model for the affinity of the peptide to the pB state (see chapter 3). Equation 1 from chapter 3 was written into IGOR Pro and was used to perform the fit. This fit yielded both the dissociation constant (K_d) and time constant (τ) for the peptide affinity.

2.4.6 Addition of BSA and lysozyme to Δ25 PYP

BSA and lysozyme were used to determine if the increase in the Δ25 PYP pB decay rate caused by the peptide is specific for the N-terminal peptide, or if the addition of any peptide or protein speeds up the pB decay rate. In these measurements, 0-5 mM of a small protein, lysozyme (14.3 kDa) was used, and 0-1 mM bovine serum albumin (66.5 kDa) was chosen for a larger protein. Samples (200 μL) of Δ25 PYP with BSA or lysozyme were placed in a 96-well plate, bleached with blue light, and the kinetics of pB decay was monitored at 442 nm.

2.4.7 Addition of Hofmeister salts and structure inducing/decreasing agents to Δ25 PYP

Because the CD spectrum of the peptide indicated only a low level of α-helical content we attempted to modulate the amount of structure in the N-terminal peptide by the addition of structure-inducing and structure-decreasing agents to Δ25 PYP. We added 0.5 M salts according to their designation (kosmotropic or chaotropic) in the classical Hofmeister series. Kosmotropic ions cause the folded state of proteins or peptides to be more stable and less soluble in water, while chaotropes have the opposite effect. Therefore, we thought that kosmotropes would induce structure and chaotropes would decrease structure in the peptide.

Ammonium sulfate and trifluoroethanol were used to increase the amount of structure in the peptide while urea and guanidinium-Cl were used to decrease the amount of structure in the peptide. Ammonium sulfate was added to Δ25 PYP in the concentration range 0-4 M. Urea was added at 0-6M and guanidinium-Cl was used in the 0-6 M range. Trifluorethanol was added from 5-15% v/v

The following 0.5 M Hofmeister salts (Table 2.2) were added to Δ25 PYP alone or Δ25 PYP with 1 mM peptide. The sodium and chloride salt of each additive was used to determine whether cations or anions have a more significant effect on Δ25 PYP pB decay rate. The samples (200 μL) were placed into a 96-well plate, bleached with blue light, and the kinetics of pB decay was monitored at 442 nm. The kinetic data were analyzed in IGOR Pro.

Chloride salts (Cl^-)		**Sodium salts (Na^+)**	
Ammonium	NH_4^+	Citrate	$C_6H_5O_7^{3-}$
Potassium	K^+	Sulfate	SO_4^{2-}
Sodium	Na^+	Phosphate	PO_4^{2-}
Lithium	Li^+	Acetate	$CH_3O_2^-$
Calcium	Ca^{2+}	Chloride	Cl^-

Table 2.2: Salt additives used with Δ25 PYP. A list of the 0.5 M sodium or chloride salts added to Δ25 PYP.

2.4.8 Δ25 PYP pH titration kinetics with peptide and citrate

For pH titration kinetic experiments the sample groups were Δ25 PYP in 50 mM MOPS buffer only, Δ25 PYP with 1 mM peptide, Δ25 PYP with 100 mM citrate, and Δ25 PYP with both 1mM peptide and 100 mM citrate. The samples contained 10 μM Δ25 PYP for all groups. All samples had their pH adjusted prior to mixing together using either 5 N HCl or 5 N NaOH, and the pH was verified again after mixing. Samples were added to a 96-well plate, bleached with blue light, and the kinetics of pB decay was monitored at 442 nm. The rate values of pB decay as a function of pH for each sample was plotted in IGOR Pro.

2.4.9 Peptide and citrate effect as a function of pH

We calculated the peptide effect and citrate effect by computing the ratio of pB decay rates with and without peptide or citrate respectively. However, the pH values

between groups were not exactly the same, and therefore the experimental data points had to be interpolated to determine the decay rate at a particular pH value. The data followed a bell-shaped curve but did not fit to a Gaussian equation. However, by using a Sigmoidal fit to each side of the bell curve the data could be fit and the peptide and citrate effect as a function of pH was determined.

2.5 Isoelectric points of the N-terminus and PAS core of various PYPs

A group of 33 PYPs spanning the phylogenetic tree of the PYP family were selected and their amino acid sequences were aligned with *H. halophila* PYP. The isoelectric points (pI) for the full-length, N-terminal region, and PAS core were determined from the amino acid sequence of each respective PYP using an online calculator from Expasy (http://web.expasy.org/compute_pi/).

2.6 Net charge of N-terminus and PAS as a function of pH

The amino acid sequences of the N-terminal region and PAS core of full-length PYP were input into the Scripps Research Institute Protein Calculator (http://protcalc.sourceforge.net/) v3.4 in order to calculate the predicted charges of each PYP region as a function of pH. Parameters were set to calculate the charges at a 0.1-pH step interval in the pH range 0-14. The values were plotted in IGOR Pro to examine charge-charge interactions between these two regions in PYP.

CHAPTER III

THE EFFECT OF THE N-TERMINAL HELICAL EXTENSION ON SIGNALING KINETICS IN PHOTOACTIVE YELLOW PROTEIN IS DOMINATED BY NON-SPECIFIC ELECTROSTATIC BUT DIRECTIONAL MOLECULAR COLLISIONS

Danny Maples[1], Masato Kumauchi[2], Wouter D. Hoff[1,2*]

[1]Department of Chemistry, and [2]Department of Microbiology and Molecular Genetics, Oklahoma State University, Stillwater OK 74078

3.1 Abstract

Stimulus-induced release of helical elements attached to a PAS core is a recurring feature in PAS domain signaling. Photoactive yellow protein (PYP) is a bacterial PAS domain photoreceptor and model system for such conformational dynamics. Deletion of the N-terminal 25-residue helical extension in PYP slows down the decay of the pB signaling state in the PYP photocycle ~1850-fold. Here we explore the mechanism by which the N-terminal region facilitates pB decay. The addition of a synthetic peptide corresponding to the N-terminal 25 residues to the Δ25 PYP mutant accelerates pB decay, but only by a factor ~4 and with poor peptide affinity (~10 mM). The strong pH-dependence of this peptide effect implies a key role for electrostatic interactions between the negatively charged N-terminal region and the positively charged PAS core, a conserved feature in the PYP family. Our results imply a critical role for the covalent

tethering of the N-terminal region by increasing local concentration and by causing directional collisions that avoid non-productive associations. Unexpectedly, attachment of an N-terminal His-tag to Δ25 PYP accelerates pB decay, implying low sequence specificity for the functioning of the N-terminal region. Progressive deletion of the N-terminal extension indicates that its secondary structure only modestly affects pB decay. These results imply that the strong variation in pB decay kinetics observed in the PYP family results mainly from substitutions in the PAS core, and that non-specific but directional and electrostatically guided molecular collisions between the N-terminal extension and the PAS core control PYP signaling kinetics.

3.2 Introduction

A major recent development in the molecular life sciences is the determination of the amino acid sequences of large numbers of proteins due to dramatic improvements in DNA sequencing technology. Sensitive methods to identify weak amino acid sequence similarities have revealed that many proteins contain short (~100 residues) conserved domains[2, 3], and that shuffling of such domains is important in protein evolution[1]. These conserved domains form large protein superfamilies that share a common three-dimensional fold, but that are highly diverse with respect to both amino acid sequence and functional properties. In many cases a linker region joins such conserved domains to other conserved domains in the same protein[6]. Initially the functional properties of such proteins were largely considered based on the function of each of the conserved domains. However, recent evidence has started to emerge indicating that the linker regions are of great functional importance, sparking research in the mechanism by which such linkers

act[4, 5]. Here we examine these questions in photoactive yellow protein (PYP), a member of the PAS domain superfamily.

The PAS domain is a ubiquitous protein module involved in a wide range of regulatory and sensory functions in all domains of life[12], and provide a rich and well-studied example of a protein superfamily. Over 50,000 proteins have been identified in the protein sequence database as contain a PAS domain, with 43 PAS domains present in the human genome[3]. The term PAS is based on the first letter of the name of the three founding members of the superfamily: the *Drosophila* clock protein Period (Per), the aryl hydrocarbon receptor nuclear translocator protein (Arnt) and the *Drosophila* single-minded protein (Sim). PAS domains have been identified in a wide range of signaling proteins[12, 13], including transcription factors, circadian clock proteins, phytochrome, and other proteins involved in regulation, photosensing, and oxygen/redox sensing. Interestingly, all members of this diverse set of proteins appear to be involved in sensing or regulation.

PYP is a blue light receptor from the halophilic photosynthetic proteobacterium *Halorhodospira halophila*[28, 40, 41], and is a prototype PAS domain[27, 42]. PYP was the first PAS domain for which the three-dimensional structure was reported[24, 43], and remains the PAS domain that is best understood in terms of biochemistry and biophysics at the protein level[42, 44]. PYP exhibits a light-triggered photocycle[40, 45] based on its *p*-coumaric acid (*pCA*) chromophore[21, 22]. Photoexcitation causes the conversion of the initial pG dark state of PYP into the long-lived pB state. The pB state has a blue-shifted absorbance spectrum and is partially unfolded[31-34, 46, 47].

A theme emerging from studies on a number of different PAS domains is the functional importance of N-terminal or C-terminal α-helical extensions. The N-terminal 25 residues of PYP contain two α-helices that are packed against the central β-sheet in the PAS core of PYP (Fig. 3.1A). The partial or complete deletion of this region causes a strong reduction in the rate of the last step in the light-triggered photocycle of PYP (Fig. 3.1B)[7, 8]. The C-terminal helical extensions of a PAS domain from the plant LOV-based photoreceptor phototropin (the Jα helix)[9] and the *Drosophila* clock protein Period[10] and the N-terminal extension of a PAS domain in the fungal photoreceptor Vivid[11] all pack against the PAS core of the protein in a position similar to that of the N-terminal region of PYP. Functionally important conformational changes have been reported to occur in all of these extensions, including the stimulus-induced release and partial unfolding of the helical region[7-11]. For PYP the release of the N-terminal region from the remainder of PYP during the photocycle has been reported[8, 36, 37]. In the case of LOV a C-terminal helical coiled-coil has been proven to be valuable for the design of novel light-regulated Histidine kinases for optogenetic applications, and involve a rotational motion in the coiled-coil results in the functional coupling of the LOV and kinase domains[48]. In general, these observations lead to the proposal that linker regions attached to PAS domains can both functionally and physically connect the PAS domain to other regions of the same protein. However, in most cases in is not clear how structural changes in the linker result in inter-domain signal relay. In addition, while a number of reports have been published on the altered properties of N-terminally truncated or altered variants of PYP[7, 8, 36-39, 46], the mechanism by which the N-terminal helical extension greatly accelerates the final photocycle step remains largely unknown. Here we report

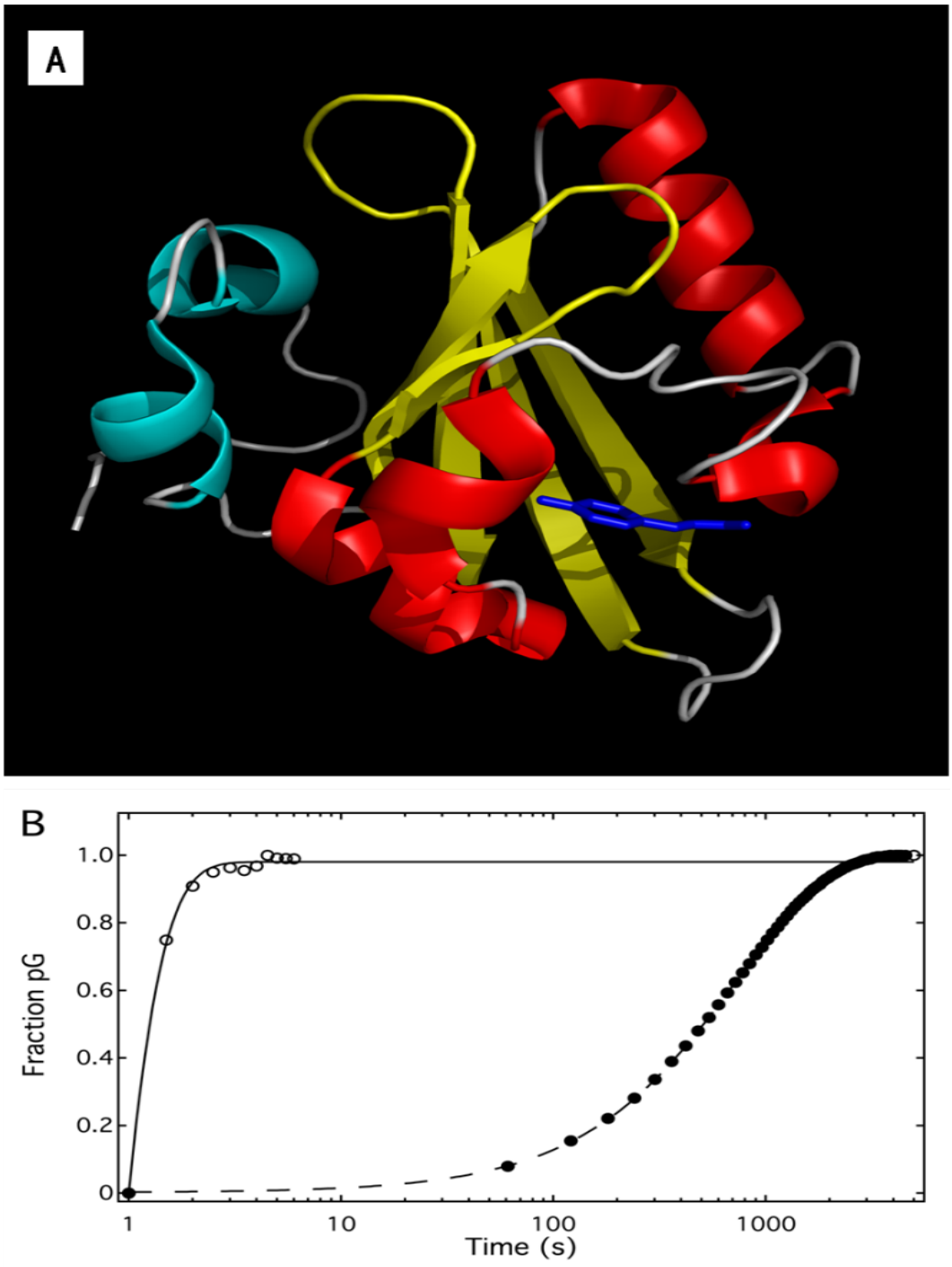

Figure 3.1: **Effect of deletion of the N-terminal helical extension on the kinetics of pB decay in Hhal PYP**. (A) Crystal structure of wild type PYP (1NWZ) from *Halorhodospira halophila* showing the location of the N-terminal region (in light blue) containing two α-helices in relation to the *pCA* chromophore (blue) and PAS core (with α-helices in red and β-strands in yellow). (B) Kinetics of pB decay (monitored using absorbance at 445 nm) for full-length PYP (solid line and open circles) and its Δ25 mutant (dashed line and filled circles), both without N-terminal His-tag.

unexpected features in the molecular mechanism that allows the N-terminal region to accelerate signaling kinetics in PYP.

3.3 MATERIALS AND METHODS

3.3.1 Mutagenesis and protein purification.

PCR using 5'-GACGACGACAAGATGGCCTTCGGCGCC-3' as the forward primer and 5'-GAGGAGAAGCCCGGTCTAGACGCGCTTGACGAAGAC-3' as the reverse primer, and wild type PYP (full-length) in pQE-80L plasmid as a template was used to create the truncated (Δ25) PYP gene. After T4 DNA polymerase treatment, the insert was annealed to pET-46 Ek/LIC vector to encode an N-terminal hexa-histidine tag and enterokinase (Ek) cleavage site for tag removal. The resulting plasmid was transformed into *E. coli* GigaSingles (Novagen). Plasmid DNA was purified using a QIAPrep Spin Miniprep Kit (QIAGEN) and sequenced to confirm truncation, histidine tag, and Ek cleavage site. The plasmid was then transformed into *E. coli* BL21 (DE3) cells grown on Luria Burtani (LB) agar plates supplemented with 100 μg/mL ampicillin. Expression of Δ25 *apo*-PYP was induced with 1 mM IPTG in LB medium containing 100 μg/mL ampicillin, and the protein was extracted from the cells using 8 M urea. After 2-fold urea dilution, the protein was reconstituted with 4-hydroxycinnamic anhydride and dialyzed against 50 mM MOPS, pH 7.5. Δ25 PYP was purified using Ni-NTA (MCLAB) affinity chromatography and anion exchange chromatography using a DEAE-Sepharose CL6B column (GE Healthcare) to a purity index (PI) = 0.46 (A_{278}/A_{442}). The tag was subsequently removed using enterokinase (New England BioLabs) and used with or without additional purification by gel filtration. The final PI was ~ 0.5.

The synthetic N-terminal peptide MEHVAFGSEDIENTLAKMDDGQLDG-amide (100 mg) was purchased from Genemed Sythesis Inc. (San Antonio, TX) as a white lyophilized powder. Peptide purity was >95% with an average mass 2722.4 amu (calculated: 2722.94 amu). The peptide was dissolved in 50 mM MOPS, pH 9 and subsequently adjusted to pH 7.5 using 5 N NaOH, to yield a 50 mg/mL concentration.

3.3.2 Absorbance spectroscopy

Transient absorption data were measured using an HP-8453 (Hewlett-Packard) diode array UV-Visible spectrophotometer and a Synergy HT Multi-Detection Microplate Reader (Bio-Tek Instruments). A 150 W halogen quartz light source (Cuda) with optical fiber light guide and a broadband blue filter (band-pass filter 59855, Oriel) was used to initiate the photocycle. Room temperature Δ25 PYP in 50 mM MOPS (pH 7.5), with or without 25-mer peptide, was placed in a 10 mm path length cuvette (and in some cases a 1 mm path length cuvette) and illuminated with blue light until steady-state pB formation. The microplate reader was used to simultaneously measure multiple samples with slow pB decay kinetics. Briefly, 200 μL of Δ25 PYP with or without 25-mer peptide was placed into wells of a 96-well plate. The plate was placed into the instrument plate holder and the wells were illuminated with blue light for about 2 minutes until steady state bleaching of the protein samples. The plate reader door was immediately closed and absorbance measurements at 442 nm were initiated and continued until completion of the photocycle. Absorption spectra at 442 nm as a function of time were collected in the dark to monitor pB decay. The data were analyzed in IGOR Pro version 6.2 (Wave Metrics, Inc) to obtain pB decay rates. For the samples analyzed

here the process of pB decay was found to be monoexponential except when stated otherwise.

To analyze the effect of the addition of the N-terminal peptide to Δ25 PYP on pB decay kinetics in terms of the affinity of the N-terminal peptide for binding to the pB state of Δ25 PYP, we use the pre-equilibrium kinetic model depicted in Scheme 1. This description assumes that the time scale for reaching the equilibrium for the formation of the complex between the N-terminal peptide and Δ25 PYP is fast compared to the pB decay rates of Δ25 PYP alone or the Δ25 PYP-peptide complex. Since the time constant for pB decay in Δ25 PYP is 740 seconds, this assumption is reasonable. This rapid equilibrium leads to a "pre-equilibrated pool" that maintains its equilibrium as it decays. Since the decays are each first-order, the overall decay kinetics of the equilibrated pool will also be first-order, with an effective rate constant that is intermediate between the individual decay rate constants. This approach results in Equation 1 for describing the effect of increasing the concentration of N-terminal peptide on pB decay in Δ25 PYP.

Scheme 1:

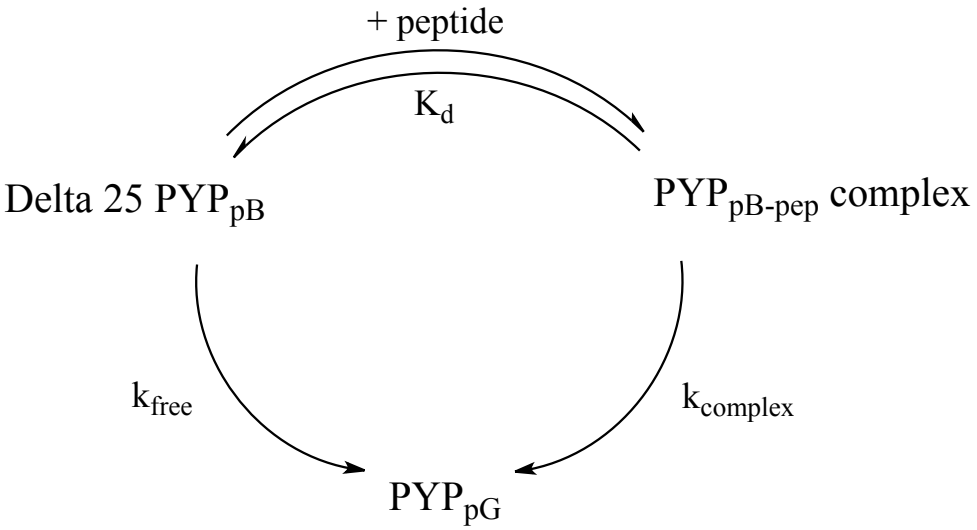

Equation 1:

$$k_{obs} = \left[\left(\frac{1}{\frac{[peptide]}{K_d}+1}\right) k_{free}\right] + \left[\left(\frac{1}{\frac{K_d}{[peptide]}+1}\right) k_{complex}\right]$$

Scheme 1 and Equation 1: Kinetic model and equation used for the affinity of the N-terminal peptide for Δ25 PYP.

The effect of the addition of the N-terminal peptide to Δ25 PYP on the lifetime of the pB photocycle intermediate was determined at a range of different pH values. In these experiments the exact pH of each sample was determined just before the spectroscopic determination of the kinetics of pB decay. To derive the change in pB life time caused by the addition of the N-terminal peptide as a function of pH, we interpolated the dependence of pB life time on pH using the following approach. The pH dependence of pB lifetime was observed to be roughly bell-shaped. A sigmoidal equation was fit to each side of the data in order to obtain pB decay values at identical pH values for data sets with or without N-terminal peptide. These interpolated data were used to obtain the peptide effect on pB lifetime as a function of pH.

3.3.3 Circular dichroism of the N-terminal peptide

The circular dichroism (CD) spectrum of the free N-terminal peptide was obtained from 190-260 nm for a 0.2 mg/mL peptide solution in 20 mM sodium phosphate (pH 7.3) using a JASCO J815 spectrometer. The K2D3 server (http://k2d3.ogic.ca/) was used to determine the secondary structure content of the peptide based on these experimental data.[49] In addition, the AGADIR server (http://agadir.crg.es/) was used to predict the helical content of peptides with a specific amino acid sequence.

3.3.4 pH dependence of charge

The pH dependence of charge for the N-terminal peptide and all PYPs and their PAS cores were calculated from their amino acid sequences using Protein Calculator v3.4 server (http://protcalc.sourceforge.net/) using a 0.1 increment step in pH, over the pH range 0-14.

3.4 RESULTS AND DISCUSSION

3.4.1 The N-terminal peptide specifically but modestly accelerates pB decay in Δ25 PYP

While the deletion of the N-terminal region of PYP alters its spectroscopic and kinetic properties, both the X-ray[38] and the solution NMR structure[46] of the pG state of the Δ25 PYP mutant revealed that the structure of the PAS core of PYP is essentially unchanged. This prompted us to explore an experimental strategy in which a synthetic peptide corresponding to the N-terminal 25 residues of full-length PYP is added to Δ25 PYP. We employed two spectroscopic readouts to probe binding of the N-terminal peptide to Δ25 PYP: the rate of pB decay and the absorbance maximum of the pG state. N-terminal deletions of PYP slow down the rate of pB decay: the lifetime of the pB state τ_{pB} of ~0.3 seconds in full-length PYP[40] is greatly increased in both Δ23 PYP (τ_{pB} ~590 seconds[7]) and Δ25 (τ_{pB} ~250 seconds[8]). Productive binding of a synthetic N-terminal peptide to the pB state of Δ25 PYP would thus be detected as an acceleration of the photocycle. In addition, the deletion of the N-terminal region of PYP blue-shifts the absorbance maximum of the initial pG state of PYP from 446 nm to 442 nm[7, 8] (Fig. 3.2A). This shift in visible absorbance maximum provides a spectroscopic tool to probe binding of the N-terminal peptide to the pG state of Δ25 PYP.

In initial experiments aimed at detecting the binding of the N-terminal peptide to the pG state of Δ25 PYP we did not observe a change in absorbance maximum upon the addition of the peptide. Therefore, we performed measurements near maximal solubility of the N-terminal peptide and Δ25 PYP. The addition of 10 mM N-terminal peptide to 1 mM Δ25 PYP (measured in a 1 mm path length cuvette) left the absorbance maximum unchanged

(Fig. 3.2B), implying that the affinity of the peptide for the pG state is substantially lower than 10 mM.

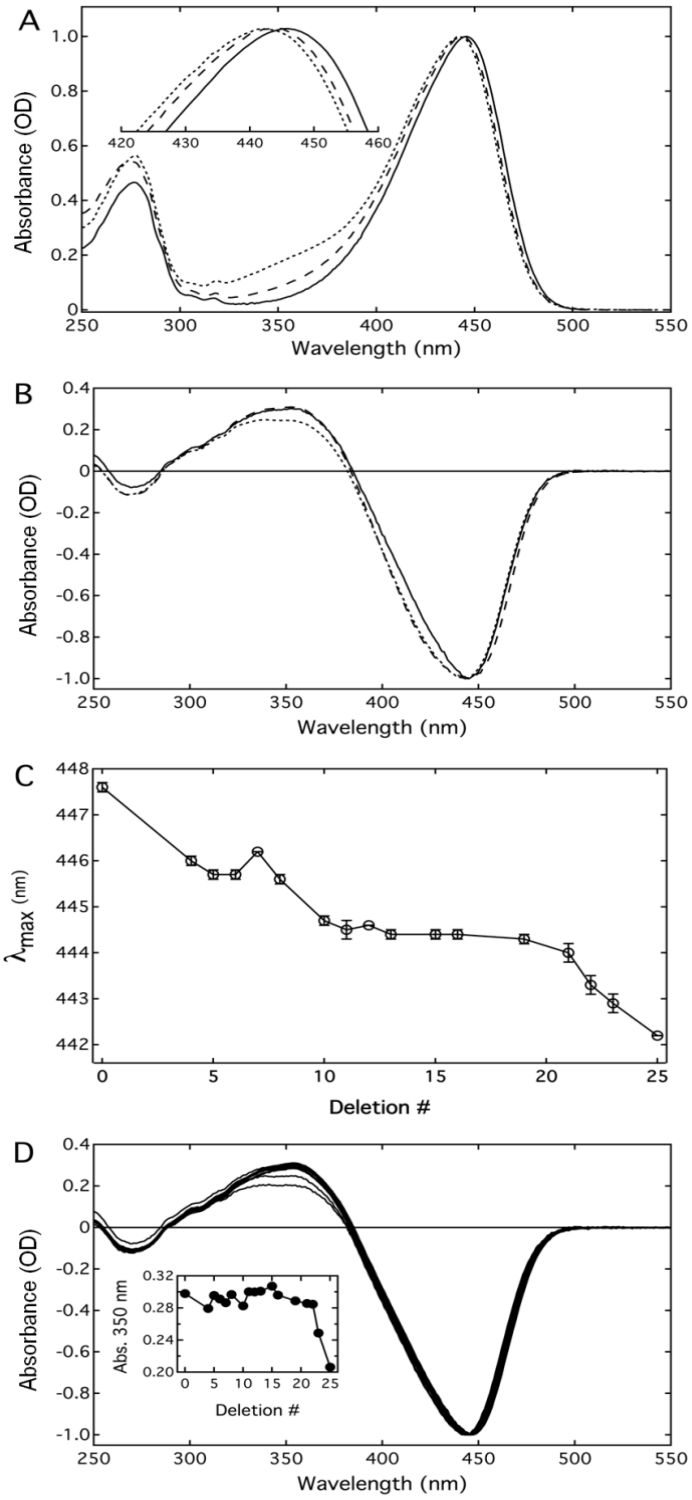

Figure 3.2: **Effect of N-terminal deletions and the addition of the synthetic N-terminal peptide on the absorbance maxima of the pG and pB state of PYP**. (A) Absorbance spectra of purified full-length HhaI PYP (solid line), the Δ25 PYP mutant (dotted line), and Δ25 PYP containing an N-terminal His tag (dashed line). The inset shows the absorbance peaks. (B) The amplitude-normalized pB – pG absorbance difference spectrum of wt PYP (solid) compared to that of 1 mM Δ25 PYP without (dotted) and with 10 mM N-terminal peptide (dashed). (C) Effect of progressive deletion of the N-terminal region on the absorbance maximum of the pG state of PYP. (D) The pB – pG absorbance difference spectra of the N-terminal deletion mutants depicted in panel C. The inset depicts the amplitude of the positive band at 350 nm caused by the population of the pB state for the series of progressive N-terminal deletion mutants.

Since the deletion of the N-terminal region of PYP slows down the decay rate of the pB intermediate by a factor ~1850, we examined if the addition of a synthetic peptide corresponding to the first 25 N-terminal residues of PYP accelerates pB decay in Δ25 PYP. We titrated increasing amounts of the N-terminal peptide to a 10 μM solution of PYP and measured the rate of the pB to pG transition after photoexcitation of the sample. Our expectation was that the addition of sufficiently high concentrations of N-terminal peptide to Δ25 PYP would restore the pB decay rate of full-length PYP. We refer to the ratio of the rates of pB decay in the absence and presence of the N-terminal peptide of PYP as the peptide effect on pB decay. Under the buffer condition used here the pB life times of full-length and Δ25 PYP and are 0.4±0.06 and 740±10 seconds, respectively. Therefore, at saturating N-terminal peptide concentrations we anticipated a maximal peptide effect of 740/0.4 = 1,850.

Measurements of the effect of the addition of the N-terminal peptide to Δ25 PYP indeed revealed a reduction in the lifetime of the pB intermediate (from 740±10 s to 184±1 s) (Fig. 3.3A). However, even at a very high peptide concentration of 15 mM, the rate of pB decay is still ~460-fold slower than in full-length PYP. The dependence of pB decay rate on the concentration of the N-terminal peptide could be described using a model (see equation 1) in which the rate of equilibration of the peptide–Δ25 PYP complex is assumed to be fast compared to the rate of pB decay, yielding a derived binding constant K_D of 9.7 ± 0.5 mM (Fig. 3B). Apparently, the affinity of the N-terminal peptide is higher for the pB state of Δ25 PYP than its pG state. However, the value of 9.7 mM is surprisingly high in view of the nano- to micromolar binding affinity found for many protein-protein interactions involved in signal transduction, including the binding

of transducing to rhodopsin[50] in vision and the binding of CheA to the flagellar motor switch in bacterial chemotaxis[51]. Extrapolation to infinite peptide concentration yields a pB life time of 121 s, corresponding to a maximal peptide effect of 6.1. This value is ~300-fold lower than the expected maximal peptide effect.

To examine the possibility that the relatively small degree of acceleration of pB decay is due to the poor affinity of the peptide for Δ25 PYP, we measured the effect of the addition of 10 mM peptide to a 1 mM solution of PYP. In this case a peptide effect of 3.5 was observed, very similar to the peptide effect of 3.7 that we measured to a 10 μM solution of PYP. These results show that the N-terminal peptide indeed has the expected effect of accelerating pB decay, but only has a modest effect on the observed rate, while binding of the peptide to Δ25 PYP occurs with poor affinity.

To determine if the acceleration of pB decay is specific for peptides corresponding to the amino acid sequence of the N-terminal region of PYP, we measured the effect of the addition of two proteins (BSA and lysozyme) on the kinetics of pG recovery (Fig. 3.3C). In the case of lysozyme no effect on pB decay rate was observed even in the presence of 5 mM added protein. For BSA a slight deceleration of pB decay was detected. We conclude that the acceleration of pB decay upon the addition of the N-terminal peptide is a specific effect that cannot be achieved by the addition of high concentrations of unrelated proteins, and therefore is related to the function of this region of native PYP.

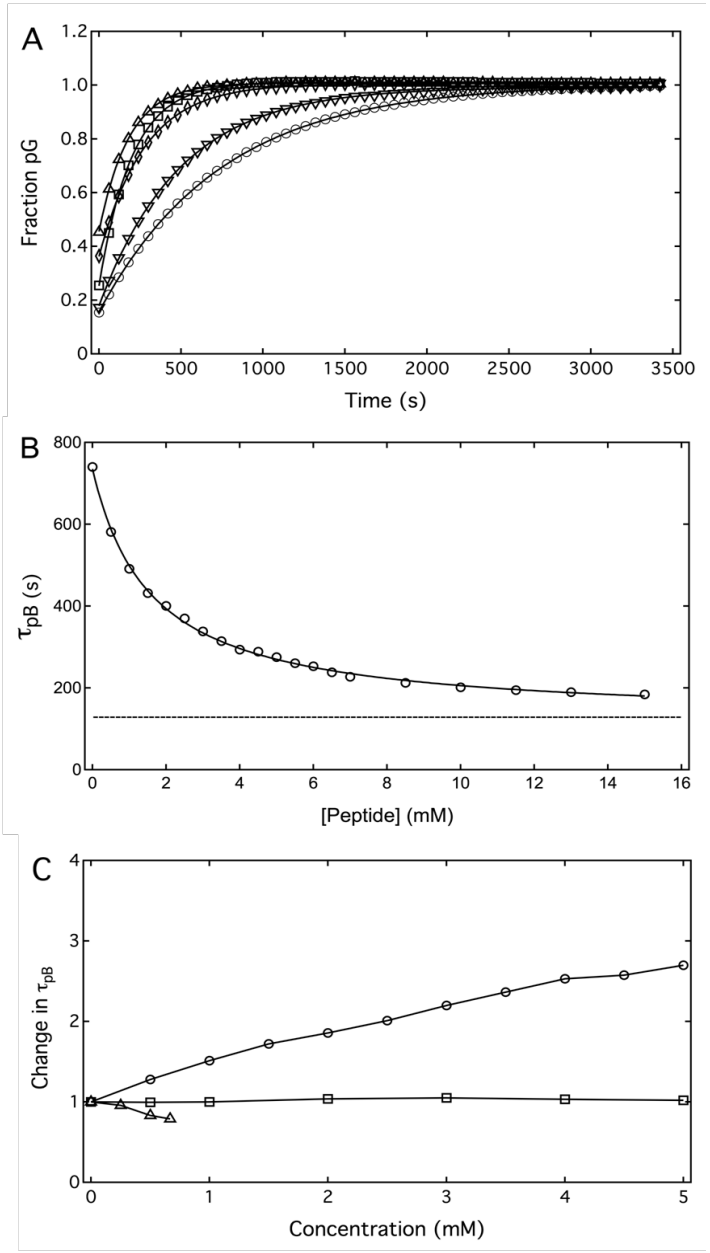

Figure 3.3: Addition of the N-terminal peptide of PYP to Δ25 PYP modestly but specifically accelerates pB decay. (A) Thermal decay of the pB intermediate to the pG state in a 10 μM solution of Δ25 PYP (pH 7.4) as monitored through absorbance at 442 nm in the absence of a synthetic peptide corresponding to the N-terminal residues of full-length PYP (open circles), and in the presence of increasing amounts of N-terminal peptide: 1 mM (downward triangles), 5 mM (open diamonds), 10 mM peptide (open squares), and 15 mM peptide (upward triangles). This resulted in pB life times of 745, 494, 278, 200, and 182 seconds, respectively. Solid lines indicate fits as a monoexponential decay. (B) The dependence of the time constant for pB decay at 20 different peptide concentrations can be described as a binding event of the peptide to the pB state of Δ25 PYP with a dissociation constant of 9.7 ± 0.5 mM. The lifetime of pB extrapolated to infinite peptide concentration (122 seconds) is depicted by the dashed line. (C) Effect of the addition of BSA (triangles), lysozyme (squares), and synthetic N-terminal peptide (circles) on altering the kinetics of pB decay in Δ25 PYP.

3.4.2 Low helical structure content in the N-terminal peptide does not explain the small peptide effect

To better understand the peptide effect, we examined the degree to which it adopts secondary structure in solution. While in the crystal structure of the pG state this region contains two α-helices (with a combined length of 9 residues), the peptide CD

spectrum of the N-terminal peptide by itself at pH 7.3 (Fig. 3.4A) shows that it is largely unstructured. Analysis of this spectrum using the K2D3 server yields an α-helical content of 14.7% and a β-sheet content of 3.7%. The helical content prediction using AGADIR is even lower (3%). For comparison, the α-helical content of this region in the crystal structure of the pG state of PYP is 35%; for the solution structure determined by NMR spectroscopy the helical content of the N-terminal region is ~20%. This raises the possibility that the tethering of the N-terminal peptide to the remainder of the protein in full-length PYP could increase the amount of secondary structure in this peptide.

To examine if the low level of structure in the N-terminal peptide is responsible for the small value of the peptide effect, we used kosmotropes and chaotropes in an attempt to modulate the amount of helical structure in the peptide. Our expectation was that the addition of kosmotropes would increase the amount of structure in the peptide, thereby enhancing the peptide effect. Conversely, the addition of chaotropes would decrease the value of the peptide effect. To reduce the degree of structure in the N-terminal peptide we used 1 M urea and Gdm-HCl; to increase its structural content we added 1 M ammonium sulfate and 0.7 M (a 5% solution) trifluoroethanol (TFE). TFE is of particular interest because it has been reported to increase α-helical structure[52]. We first determined the effect of the addition of these compounds on the rate of pB decay in Δ25 PYP in the absence of added N-terminal peptide, and observed that TFE and urea slow down pB decay (by a factor 1.3 and 1.23, respectively) while Gdm-HCl and ammonium sulfate speed up pB decay (by a factor of 1.45 and 4.3, respectively)(Fig. 3.4B). The effect of the addition of 1 mM peptide on pB decay rate (1.5 in the absence of

additives) is slightly reduced by the addition of TFE, urea, and Gdm-HCl (down to 1.0), and is somewhat increased by the addition of ammonium sulfate (to 2.02)(Fig. 3.4C).

A detailed interpretation of the effect of these additives on the peptide effect is complex because their effects can be caused through changes in the structure of the peptide or changes in the structure of the pB state (or a combination of these two effects). The magnitude of the effects of the additives on the rate of pB decay in Δ25 PYP are similar to their influence on the peptide effect. We tentatively conclude that the expected changes in the degree of helical content of the N-terminal peptide caused by the additives only have a minor influence on the magnitude of the peptide effect. This result argues against the notion that the low level of structure in the N-terminal peptide is the cause of the relatively small effect of its addition to Δ25 PYP.

Because we observed that kosmotropes and chaotropes alter the value of the effectiveness of the N-terminal peptide in accelerating pB decay, we examined if this effect follows a Hofmeister series. These experiments also build on the recently reported result that the kinetics of the photocycle of full-length PYP exhibits a Hofmeister effect[53, 54]. We measured the effect of adding 1 mM of the peptide to Δ25 PYP on the rate of pB decay in the absence or presence of a series of chloride salts and sodium salts, each at 0.5 M concentration. These experiments revealed that pB lifetime for Δ25 PYP in the absence of the N-terminal peptide follows a Hofmeister effect, but only for the negative ions, in which kosmotropes accelerated pB decay in Δ25 PYP. Measurements in which the N-terminal peptide was added to Δ25 PYP indicated that the effect of Hofmeister salts on the peptide effect on pB lifetime is relatively small, in line with the above results

(Fig. 3.4C) While the peptide effect in the absence of these salts is 1.5, the value ranges from 1.17 (calcium chloride) to 1.79 (sodium sulfate).

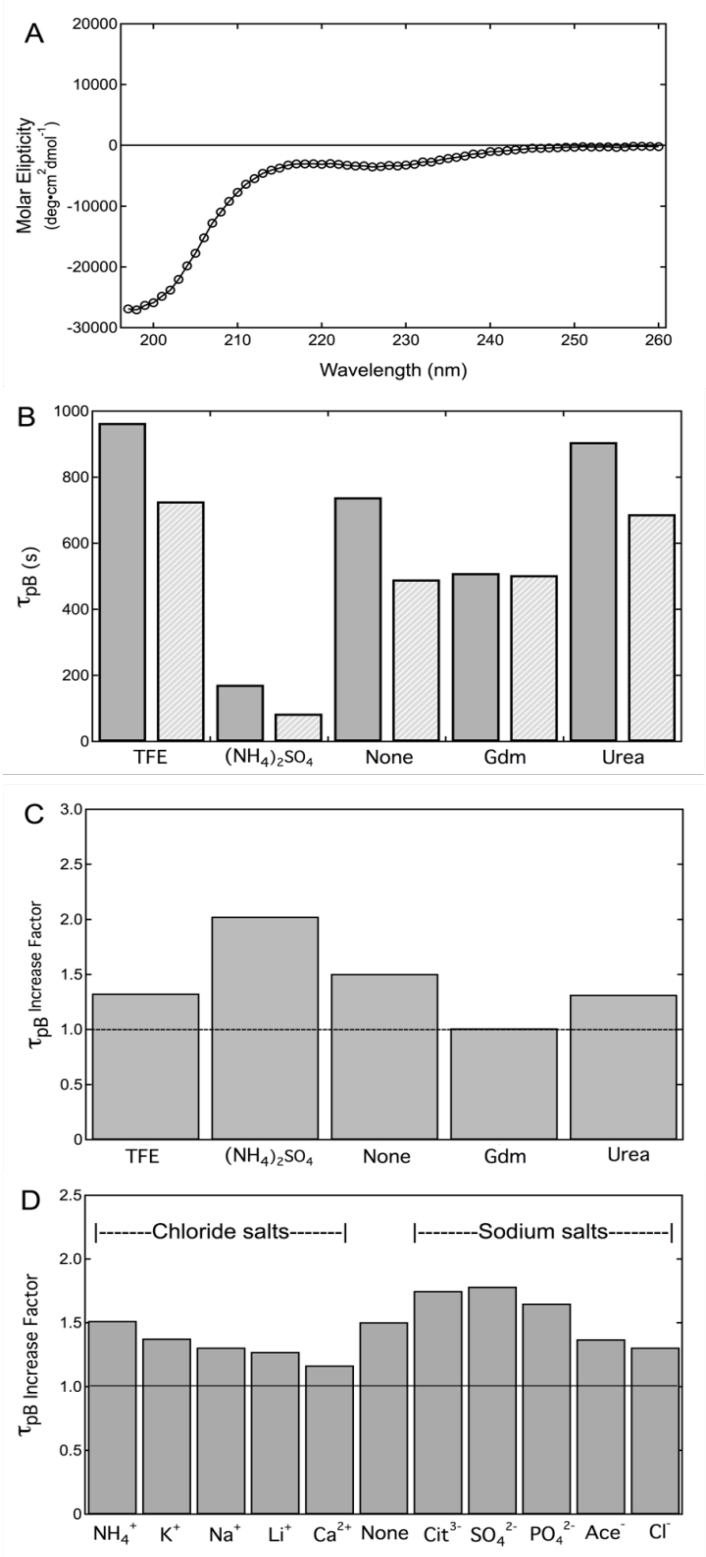

Figure 3.4: Kosmotropes and chaotropes only modestly alter the effect on pB decay of adding 1 mM N-terminal peptide to Δ25 PYP and follow the Hofmeister series. (A) The circular dichroism spectrum of the peptide corresponding to the 25 N-terminal residues of PYP indicates that this fragment is largely unstructured. (B) Effect of two kosmotropes (1 M ammonium sulfate and 5% TFE) and chaotropes (1M urea and Gdm-HCl) on the time constant for pB decay in the absence (dark gray bars) and presence (light gray bars) of 1 mM peptide. (C) Kosmotropes and chaotropes modestly alter the acceleration of pB decay in Δ25 PYP by the addition of the N-terminal peptide. (D) The peptide effect for accelerating pB decay in Δ25 PYP follows the Hofmeister series. The effects of the addition of 0.5 M of indicated potassium and chloride salts, arranged according to the classic Hofmeister series, on the value of the peptide effect on accelerating pB decay is shown.

3.4.3 Covalent tethering plays a key role in acceleration of pB decay by the N-terminal region

The finding that the addition of the N-terminal peptide only modestly accelerates pB decay in Δ25 PYP implies that an important difference exists between full-length PYP and the case in which the N-terminal region and the PAS core of PYP are no longer covalently attached. NMR studies on the pB state in full-length and Δ25 PYP indicate that the light-induced structural changes in the PAS core of PYP still occur[46]. In addition, the analysis of the effect of kosmotropes and chaotropes presented above indicates that a loss of helical structure in the N-terminal region upon its dissociation of PYP does not play a major role in the small value of the peptide effect. This leaves the covalent tethering of the N-terminal region to the PAS core of PYP as a likely candidate for greatly increasing the effect of the N-terminal region in accelerating pB decay in full-length PYP. Since the maximal peptide effect is ~6 and the peptide effect that would be needed to restore the pB decay rate to its value in full-length PYP is 1,850, an explanation is needed for a ~300-fold increase in the efficacy of the N-terminal peptide for accelerating pB decay. We consider how covalent tethering of the N-terminal peptide could contribute to this effect.

Tethering will result in a very high local concentration of the N-terminal peptide that the remainder of PYP experiences in the full-length protein. An estimate of the effective concentration[55, 56] of the N-terminal region that the remainder of PYP experiences can be estimated by considering the volume that the unstructured peptide would occupy. Taking the length of the extended N-terminal 25 residues as 25*0.38 nm = 9.5 nm, the theoretical volume of the fully extended N-terminal peptide is $4.5 * 10^5$ Å^3,

corresponding to a local peptide concentration of 3.7 mM. This local concentration effect can explain how the N-terminal region is able to strongly accelerate pB decay in full-length PYP despite its low binding affinity (K_D of 9.7 mM). Interestingly, in the case of LOV2 domain from *Avena sativa* (oat) an affinity of 17 mM for the binding of the Jα helix was found.[57] However, the local concentration effect does not explain why extrapolation to infinite peptide concentration falls short by a factor of ~300 in achieving the pB decay rate of full-length PYP.

We propose that an effect other than local concentration plays a key role in the enhancement of the peptide effect by covalent tethering: the non-random orientation of the N-terminal peptide with respect to the PAS core of PYP. Tethering of the N-terminal peptide to residue 26 in PYP can be expected to enhance the frequency of a selected set of molecular collisions between the N-terminal region and the remainder of PYP with orientations that are favored by the tethering, while reducing the chance for collisions in which the N-terminal region and PYP have other conformations. A further increase in the peptide effect of the tethered N-terminal region in full-length PYP could occur if the free N-terminal peptide can transiently interact with Δ25 PYP in both productive and non-productive conformations. Non-productive complexes would need to dissociate before a functional complex can be formed, and would thus function as a kinetic trap that reduces the effectiveness of the N-terminal region in accelerating pB decay. This proposed kinetic trap model is analogous to misfolded intermediates that slow down the rate of protein folding by acting as kinetic traps.[58, 59]

We conclude that covalent tethering of the N-terminal peptide to residue 26 in full-length PYP is critical for its effect in speeding up pB decay from ~740 seconds in

Δ25 PYP to ~0.4 seconds in full-length PYP. In this model directional molecular collisions play a key role in pB decay in full-length PYP by favoring the formation of productive complexes between the N-terminal region and the remainder of PYP, while avoiding potential non-productive conformations of the complex formed between the N-terminal region and the remainder of PYP.

3.4.4 An N-terminal cleavable Histidine tag accelerates pB decay in Δ25 PYP

To facilitate the purification of Δ25 PYP we initially worked with a construct containing an N-terminal enterokinase-cleavable Histidine tag. Unexpectedly, the presence of this affinity tag accelerated the decay of the pB state by a factor ~10 (Fig. 3.5A) and also caused a small (~1 nm) red-shift in absorbance maximum (Fig. 3.2A and supplemental Table 1). The amino acid sequence of this 14-residue affinity tag (MAHHHHHHVDDDDK) shares no similarity to the N-terminal region of PYP (MEHVAFGSEDIENTLAKMDDGQLDG), and has negligible predicted helical content.

To provide a more direct comparison of the acceleration of pB decay in Δ25 PYP caused by the attachment of the 14-residue affinity tag, we compared the photocycle kinetics of His-tagged Δ15 PYP with that of untagged Δ11 PYP. These two proteins share the same total length of 114 residues, in which 14 N-terminal residues are attached to the PAS core of PYP. Remarkably, the time constant for pB decay in His-tagged Δ25 PYP (~77 s) is smaller than in untagged Δ11 PYP (146 s) (Fig. 3.5A). Apparently, attachment of the 14-residue cleavable N-terminal affinity tag to Δ25 PYP accelerates pB decay more effectively than the native 14 N-terminal residues remaining in Δ11 PYP. These observations imply that the effect of the acceleration of the decay of the pB state by the attachment of an N-terminal peptide to Δ25 PYP exhibits a remarkably low level

of amino acid sequence. This finding is in line with the poor affinity of the N-terminal peptide for Δ25 PYP.

We also measured the effect of the covalent attachment of this affinity tag to full-length PYP, and found that in our buffer conditions the presence of this tag slows down pB decay by a factor ~1.8 (from a time constant of 0.4 seconds to 0.7 seconds) (Fig. 3.5A). Thus, the accelerating effect of the attachment of this affinity tag occurs for Δ25 PYP but not for full-length PYP.

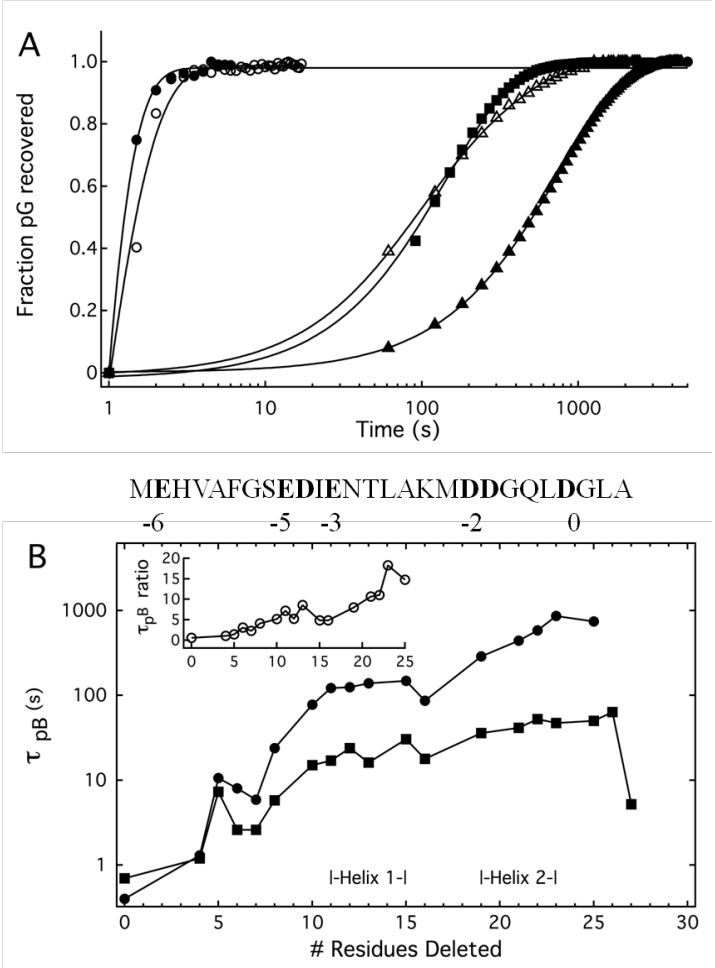

Figure 3.5: Effects on pB life time of modifying the N-terminal region of PYP. (A) The kinetics of the pB to pG transition as observed through absorbance at 446 nm is depicted for full length PYP without (black circles) and with (open circles) N-terminal affinity tag, and for Δ25 PYP without (black triangles) and with (black triangles) N-terminal affinity tag. The pB decay kinetics for Δ11 PYP without N-terminal affinity tag is also depicted (closed squares). The observed pB lifetimes for these five samples were 0.4, 0.7, 740, 77, and 122 seconds. In the case of the Δ25 PYP mutant with His tag pB decay was slightly biexponential (τ_1 = 76 s with 57% of the amplitude and τ_2 = 323 s with 43% of the amplitude). (B) An N-terminal deletion series reveals the effects of progressively deleting the first 27 N-terminal residues of PYP on pB decay kinetics in PYP in the presence (black squares) and absence (black circles) of an N-terminal His tag. The amino acid sequence of the N-terminal region is depicted immediately above this panel, with negatively charged residues indicated in bold, and with the predicted net charge of the N-terminal region at neutral pH as it is progressively shortened.

3.4.5 Progressive deletion identifies residues in the N-terminal region of PYP that contribute to the acceleration of pB decay

To better define which residues in the N-terminal region of PYP contribute to the acceleration of pB decay, we performed a systematic progressive deletion analysis of the first 27 residues of full-length PYP. This work complements published results in Δ6 PYP, Δ15 PYP, and Δ23 PYP based on proteolytic fragmentation[7] and on genetic constructs for Δ25 PYP and Δ27 PYP[8]. We prepared 18 deletion mutants ranging from Δ4 PYP to Δ27 PYP with enterokinase cleavable His-tags. Unexpectedly, we found that for Δ26 and Δ27 PYP the His-tag could not be removed even after extensive treatment with enterokinase. Attempts to promote cleavage of the tag by the addition of urea were not successful. This result implies that accessibility to the proteolytic cleavage site is eliminated upon attachment of the tag too close to the PAS core. Inspection of the crystal structure of PYP suggests that steric hindrance caused by the bulky residue F28 keeps the terminal lysine of the cleavage site from sufficiently entering into the enterokinase active site. For the remaining 16 deletion mutants the proteolytic removal of the N-terminal tag proceeded efficiently, allowing their absorbance spectra and pB decay rate to be measured.

Progressive deletion of residues from the N-terminus of PYP (without His-tag) yielded a largely monotonous increase in pB lifetime from 1.3 seconds for Δ4 PYP up to 860 seconds for Δ23 PYP, for a total of 860/0.4 = 2,150-fold increase in lifetime (Fig. 3.5B). Two exceptions to this pattern are that the pB lifetime of Δ16 PYP (89 seconds) was somewhat faster than that of Δ15 PYP (148 seconds) and that Δ25 PYP (740 seconds) was somewhat faster than that of Δ23 PYP (860 seconds). The overall pattern of

increasing pB lifetime upon progressive deletion appears to be superimposed with two step-wise increases that roughly correspond to the position of the two α-helices in the N-terminal region of PYP (Fig. 3.5B).

For PYP samples in which the N-terminal His_6-tag was not removed, the effects of progressive deletion on the rate of pB decay are smaller, gradually slowing down from 0.7 seconds in full-length PYP to 63 seconds in Δ26 PYP (a 90-fold increase in lifetime). Unexpectedly, for Δ27 PYP containing the His-tag the rate of pB decay substantially accelerated (lifetime 5.2 seconds). Comparison of the rate of pB decay in the deletion mutants in the absence and presence of the N-terminal cleavable His-tag (Fig. 3.5B) reveals that the accelerating effect of the attachment of the N-terminal His-tag occurs for all deletion mutants in the range Δ10 through Δ25 PYP. The accelerating effect of the His_6-tag became more pronounced in the progressive deletion series (inset of Fig. 3.5B). Apparently the presence of the N-terminal affinity tag diminishes the effect of deleting the N-terminal region of PYP on the kinetics of pB decay in all of the deletion mutants studied here. In line with the analysis of kosmotropes and chaotropes on the peptide effect presented above, this result implies that the acceleration of pB decay caused by the addition of this affinity tag is not sensitive to the detailed structure of the N-terminal region. In addition, this observation suggests that this affinity tag contains a sequence feature that accelerates pB decay irrespective of its exact location in the N-terminal region. Below we describe results indicating that this feature is the presence of four adjacent negatively charged residues.

In line with previous results[7, 8], we observed a slight blue-shift in the absorption maximum of the initial pG state from 446 nm to 443 nm in some of the N-terminal

deletion mutants (444 nm when the N-terminal His-tag is present). A substantial part of this shift occurs upon the deletion of residue 22 (21 when the N-terminal His-tag is present) (Fig. 3.2C). These results imply that the region formed by residues 22 through 25 substantially interacts with the PAS core of PYP, and that this interaction affects the absorption maximum of PYP. Since the *pCA* binding pocket is located on the opposite face of the central β-sheet in PYP compared to the N-terminal region, this involves indirect interactions between relatively remote regions of the protein.

3.4.6 Strong pH dependence of the peptide effect reveals the importance of electrostatic interactions between the N-terminal region and the PAS core of PYP

Since pH strongly affects the rate of pB decay in full-length PYP[60, 61], we explored the possibility that the accelerating effect of the N-terminal peptide on pB decay is pH-dependent. As a first step we determined the pH dependence of pB decay in Δ25 PYP. Unexpectedly, the pH dependence of pB decay for Δ25 PYP is opposite to that observed for full-length PYP (Fig. 6A). While for full-length PYP the time constant for pB decay is smallest near pH 8, and pB decay is slowed down at both lower and higher pH[61], in the case of Δ25 PYP pB decay is slowest near pH 7. These results indicate that the nature of the barrier for pB decay is substantially altered by the truncation of the N-terminal region. This finding is in line with previous studies on the temperature dependence of Δ25 PYP, which revealed a reduced degree of burial of hydrophobic surface area upon pB decay as reflected in a smaller activation change in heat capacity upon reaching the transition state[8].

We next measured the effect of adding 1 mM N-terminal peptide to Δ25 PYP on the rate of pB decay at various pH values in the range pH 4 to 9.5 (Fig. 3.6B). This

experiment revealed that the peptide effect on pB life time is strongly pH dependent: while the peptide effect has a value near 1.5 close to neutral pH, at pH 5.5 its value increases to ~2.3 (Fig. 3.6C). At pH 9 and near pH 4 the peptide effect decreases to zero. Thus, at pH 5.5 the addition of 1 mM N-terminal peptide speeds up pB decay by a factor 2.3, while at pH 4 and 9 the same peptide has very little effect on pB decay. These results imply that electrostatic interactions between the N-terminal peptide and the PAS core of PYP play a critical role in the mechanism by which the N-terminal peptide affects the kinetics of decay. In addition, the data suggest that the bell-shaped pH dependence of pB decay rate on pH in wt PYP, with a maximal rate near pH 8[61], may to a substantial degree be due to the pH dependence of the interactions between the N-terminal region and PAS core of PYP: both at low pH (below ~4) and high pH (above ~9) the N-terminal region is less effective in interacting with the PAS core of PYP, resulting in a reduction in the rate of pB decay. In this interpretation the groups responsible for the pH dependence of pB decay in wtPYP are ionizable groups that guide the productive interaction between the N-terminal region and the remainder of PYP.

Because a number of the observations reported here indicate a substantial degree of non-specificity in the mechanism by which the N-terminal peptide alters pB decay kinetics, we considered the role of the overall charge in the peptide effect of accelerating pB decay. Based on the amino acid sequences involved, we calculated the pH dependence of the net charge of both the N-terminal peptide and the PAS core of PYP. While such calculations do not take into account residues with pK_a values that are shifted in the folded state of the protein (such as the side chain of Glu46), overall this approach has been found to yield fairly accurate estimates of the isoelectric point (pI) of proteins[62].

For example, the calculated pI of PYP based on its amino acid sequence is 4.8, while its experimentally measured pI is 4.3[63].

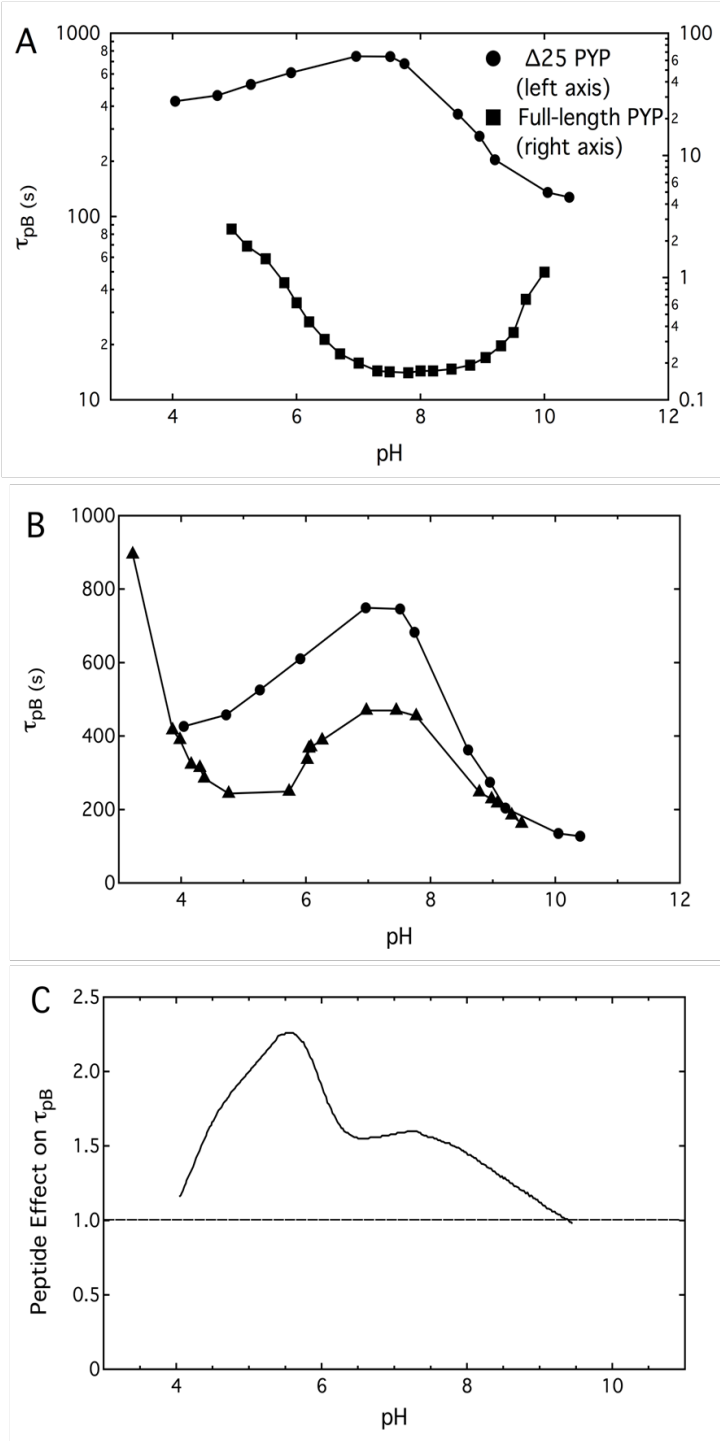

Figure 3.6: Effect of pH on the peptide effect for pB lifetime in Δ25 PYP. (A) The pH dependence of pB life time are strikingly different for full-length PYP (squares) and Δ25 PYP (circles). (B) The pH dependence of pB life time in Δ25 PYP in the absence (circles) and presence (triangles) of 1 mM N-terminal peptide. (C) The pH dependence of the peptide effect for pB decay in Δ25 PYP interpolated from the data depicted in panel C. All data are for samples without N-terminal His-tag.

This approach is therefore useful to examine if the interactions between the N-terminal peptide and the PAS core of PYP are mediated by their overall charge. Since this approach does not consider any other structural features, such as how the charge is distributed over these two parts of PYP, it provides an estimation of the effect of the overall net charge in the interaction between the N-terminal region of PYP and its PAS core.

These calculations yielded the following insights (Fig. 3.7A). At pH values below 3.9 both the N-terminal peptide and the PAS core of PYP are positively charged (due to the protonation of Glu and Asp side chains, while Arg, Lys, and His side chains are positively charged), leading to the prediction that in such acidic pH values the peptide effect will be zero because of electrostatic repulsion. At pH values between 4.1 and 7.1 the peptide is negatively charged while Δ25 PYP is positively charged. This will result in electrostatic interactions between these two fragments of PYP and therefore would allow the N-terminal peptide to accelerate pB decay. At pH values above pH 7.1 both the peptide and Δ25 PYP are negatively charged, again leading to the prediction of electrostatic repulsion and the absence of a peptide effect for pB decay. These results qualitatively agree with the experimental observation that the maximal peptide effect occurs between pH 4 and 7 (Fig. 3.6C).

The importance of negatively charged residues in the N-terminal region for accelerating pB decay provides an attractive explanation for the unexpected increase in pB decay rate upon the addition of the cleavable His_6 tag. In addition to six consecutive His residues, this tag consists of an enterokinase cleavage site containing four consecutive Asp residues, resulting in a calculated pI value for this affinity tag of 6.0.

This sequence feature raises the possibility that the strongly negatively charged region in the N-terminal affinity tag is responsible for the observed acceleration of pB decay when this tag is attached to Δ25 PYP. In this interpretation, the observation that the covalent attachment of the His tag accelerates pB decay in all progressive N-terminal deletion mutants that we tested (see Fig. 3.5B) implies that the number of amino acids separating the negatively charged region in the N-terminal region and the PAS core of PYP is not essential for its functional effect in accelerating pB decay. The data suggest that smaller number residues between the four Asp residues in the His_6 tag and residue 26 in PYP increase the extent to which the tag accelerates pB decay (see inset of Fig. 3.5B).

These considerations indicate that the negative charge of the N-terminal peptide is of considerable importance for the mechanism by which it speeds up pB decay. The N-terminal region in full-length Hhal PYP contains four Asp residues, three Glu residues, one Lys and one His, and as a result of this large excess of negatively charged residues has a calculated pI of 3.9 and a charge of -6 near neutral pH. The PAS core of Hhal PYP carries a net charge of close to zero at neutral pH. Interestingly, the removal of negatively charged residues upon progressive deletion of the N-terminal region appears to correlate with the resulting increase in pB lifetime: the first step-up in the time constant for pB decay occurs when Glu9 and Asp10 are deleted; the second step-up correlates with the deletion of Asp19, Asp20 (Fig. 3.5B).

To further examine the structural basis for the electrostatic interactions between the N-terminal region and the PAS core of PYP, we considered the distribution of charged residues on the molecular surface that forms the contact between Δ25 PYP and the N-terminal region in the pG state of full-length PYP. Interestingly, a stretch of

positively charged residues (K106, K110, K123, and potentially also His 108) with side chains pointing towards the N-terminal region is present in β-strands 5 and 6 (Fig. 3.7B). These charged residues form an attractive proposed interaction site for the negatively charged N-terminal region of PYP during the process of pB decay.

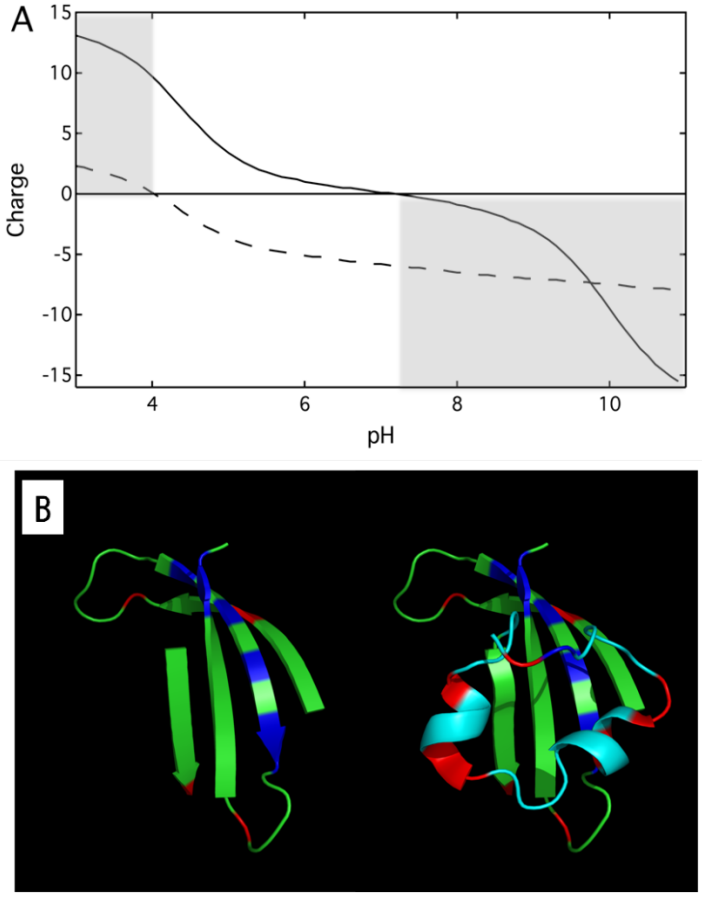

Figure 3.7: Bioinformatic analysis of the proposed role of charge-charge interactions between the N-terminal region and the PAS core of PYP during pB decay. (A) The calculated net charge of the N-terminal region (dashed line) and the PAS core (solid line) of PYP as a function of pH. The pH ranges where these two fragments of PYP both carry a positive or negative charge and thus would not experience attractive charge-charge interactions are indicated by the gray boxes. (B) Depiction of the charged residues in the PAS core of PYP onto which the N-terminal region is packed in the pG state of PYP (PDB ID 2ZOH). Positive (blue) and negative (red) residues are indicated in the PAS core (left) and PAS core with N-terminal region (right). α-helices in the N-terminal extension are shown in aqua in the right panel.

3.4.7 A charge difference between the PAS core and N-terminal region is conserved in the PYP family of photoreceptors

To examine if the electrostatic nature of the interaction between the N-terminal region and the PAS core of the PYP from *Halorhodospira halophila* plays a role in other members of the PYP family[64, 65], we selected representative PYPs across the phylogenetic tree[65] of current members of the PYP family and calculated the isoelectric point of the full length protein, the N-terminal region, and the PAS core of each PYP (Fig. 3.8). While the calculated pI of these members of the PYP family varied from 4.15 to 9.55 (average 6.53), a distinct pattern was observed for the N-terminal regions and the PAS cores of these proteins. The pI of the N-terminal regions varied from 3.33 to 5.36 (average 4.06), while for the PAS core regions the observed range was from 4.50 to 11.36 (average 8.36). All N-terminal regions (with a single exception in the case of the PYP from *Rhodomicrobium vannielii*) exhibited an excess negative charge, while most PAS cores (70%) have an alkaline pI (Fig. 3.8A). The average excess positive charge at pH 7 on the PAS core compared to the N-terminal region is 7.4 ± 3.9 (Fig. 3.8B). Therefore, in the great majority of PYPs the N-terminal region is substantially more negatively charged than the PAS core near neutral pH. Attractive electrostatic interactions between a negatively charged N-terminal region and a more positively charged PAS core appear to be a conserved feature in the PYP family of photoreceptors.

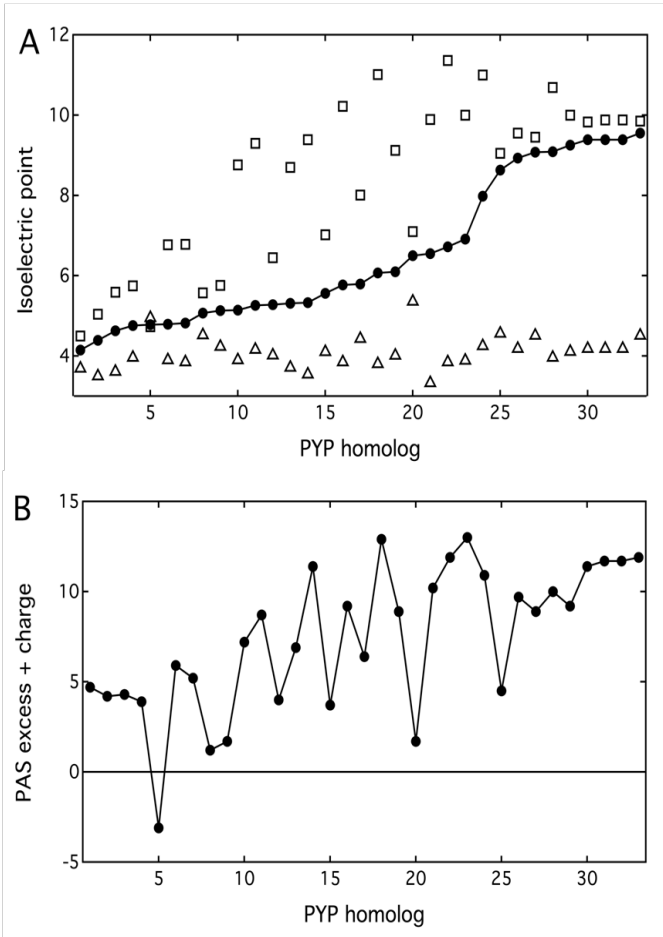

Figure 3.8: Conservation of a negatively charged N-terminal extension and positively charged PAS core in the PYP family. (A) The isoelectric point (pI) of 33 members of the PYP family (randomly selected throughout the phylogenetic three of the PYP family) was calculated and plotted from the PYP with the lowest pI to the PYP with the highest pI (filled circles and solid line). For each of these PYPs the pI of the N-terminal region (open triangles) and PAS core (open squares) was also calculated. (B) The excess positive charge at pH 7 on the PAS core compared to the charge on the N-terminal region was calculated for each of the PYPs depicted in panel A. The Hhal PYP studied in detailed here is protein number 6 in this list. The PYP from *Rhodomicrobium vannielii* (number 5) stands out as the only PYP that does not follow the observed trend.

3.4.8 Effect of citrate on photocyle kinetics and the peptide effect in Δ25 PYP

The pB state of PYP binds the dianionic form of citrate with an affinity of ~60 mM, and slows down pB decay by a factor of up to ~6 at pH 5.[66-68] The citrate binding site in PYP as identified by NMR spectroscopy is located in between the N-terminal region and the central β-sheet[66]. Because of the involvement of the N-terminal region in forming this binding site, we examined if deletion of the N-terminal 25 residues abolished the effect of citrate on pB decay rate. The addition of 100 mM citrate to Δ25 PYP resulted in a pH-dependent acceleration of pB decay (Fig 3.9A). Apparently, while the addition of citrate reduces the rate of pB decay for full-length PYP, is accelerates this

process in Δ25 PYP. As a result, citrate follows the Hofmeister series for Δ25 PYP (Fig. 3.4D). The maximal degree of acceleration of pB decay in Δ25 PYP upon citrate addition was found to be a factor 2.3 at pH 6.0. In a previous report it was found that citrate does not affect the rate of pB decay in Δ25 PYP[66]. However, in that work the His tag was not removed from Δ25 PYP. In view of the effect of the affinity tag on pB lifetime in Δ25 PYP reported above, we attribute this discrepancy in the effect of citrate on the rate of pB decay in Δ25 PYP to the presence or absence of this tag.

We also determined the effect of the presence of 100 mM citrate on the degree of acceleration of pB decay caused by the 1 mM of the N-terminal peptide to Δ25 PYP (Fig. 3.9B). In the pH range 4.6 to ~8 the presence of citrate reduced the peptide effect. This is particularly the case at pH 5.5, where citrate reduces the value of the peptide effect from has 2.3 to 1.1. These data indicate that citrate binds to both full-length and Δ25 PYP, and suggest that citrate binding impedes productive interactions between the N-terminal region and the PAS core of PYP. We propose the following explanation for the observation that citrate has the opposite effect on the rate of pB decay in full-length and Δ25 PYP. In the case of full-length PYP citrate hampers the acceleration of pB decay by the N-terminal region, resulting in slower pB decay. In Δ25 PYP the specific binding site for citrate is disrupted, and in this case citrate has an effect on pB decay through a Hofmeister effect, which may affect the protein hydration shell[69] and apparently accelerates pB decay in Δ25 PYP.

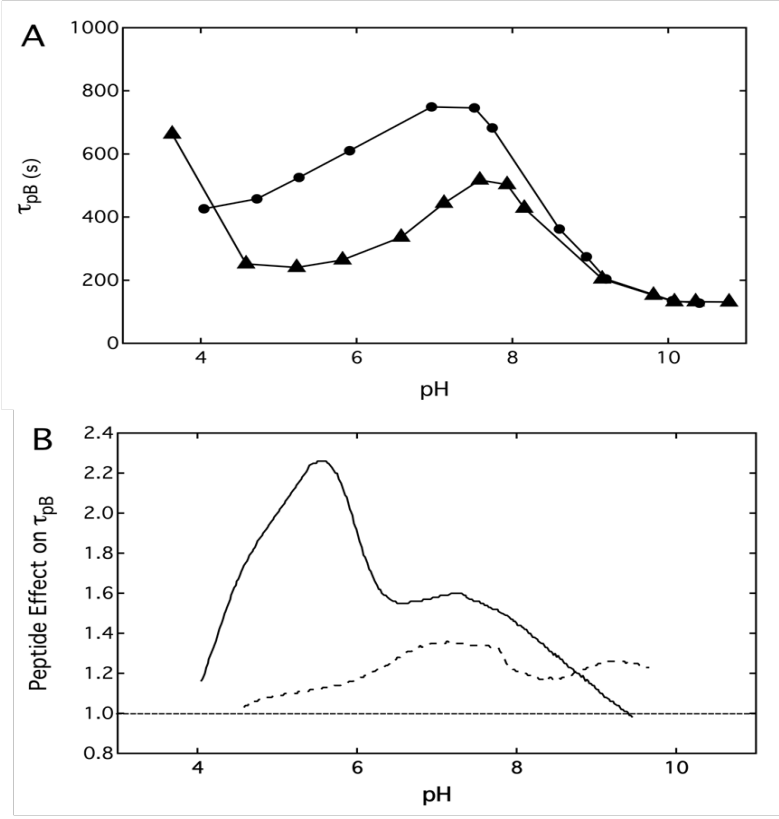

Figure 3.9: The effect of citrate on the pB decay kinetics of Δ25 PYP and its acceleration by the N-terminal peptide. (A) The pH dependence of pB decay in Δ25 PYP in the absence (circles) and presence (triangles) of 100 mM citrate. (B) The pH dependence of the value of the peptide effect on pB life time in Δ25 PYP in the absence (solid line) and presence (dotted line) of 100 mM citrate.

3.4.9 Factors that control the pB life time in the PYP family

The rate of pB decay in different members of the PYPs family of photoreceptors spans approximately 6 orders of magnitudes. In the PYP family pB life times have been reported ranging from ~1 hour for the PYP from *Salinibacter ruber*[64, 70] to ~0.3 seconds for the highly studied PYP from *H. halophila*[40], to ~1 millisecond for the PYPs from *Rhodobacter sphaeroides*[71] and *Rb. capsulatus*[72]. Because the pB state is considered to be the signaling state of PYP, its decay rate is biologically relevant[73]. Therefore, it is of considerable interest to identify the factors that result in the observed wide range of pB decay rates, both in the PYP family of photoreceptors and in mutants of Hhal PYP. Since PYP consists of a PAS core and an N-terminal extension, and because removal of this extension greatly alters the lifetime of the pB state in the case of Hal PYP, the question

arises how much of the variability in pB decay rate in different PYPs is caused by the N-terminal region.

A number of published results provide information on the role of the N-terminal region in regulating pB life time. All PYPs that have been identified thus far[65] contain an N-terminal region attached to their PAS core, indicating its biological importance throughout the PYP family. We report here that in almost all PYPs the N-terminal region is negatively charged while the PAS core is positively charged (Fig. 3.8). The pH-dependence of the accelerating effect of adding the N-terminal peptide to Δ25 PYP suggests the possibility that such interactions affect pB decay rate in many members of the PYP family. However, the rate of pB decay in a chimeric PYP consisting of the first 21 residues of the PYP from *Rb. capsulatus* attached to the remaining residues of Hhal PYP was unaffected[39]. The effect of point mutations in Hhal PYP on its pB decay rate have been studies exhaustively[74], revealing that the three point mutations in the N-terminal region that most affect pB life time are F6A, I11A, and D24A. These mutations reduce pB decay rate by a relatively modest factor of up to ~50[74, 75]. In contrast, point mutations in the PAS core of Hhal PYP have been reported that greatly affect the rate of pB decay. In the case of Hhal PYP the N43A, F96A, and M100A mutations slow down pB decay by 3 orders of magnitude[73, 76-78], while the E46Q mutation accelerates pB decay by a factor ~30[61]. Taken together, these observations do not provide support for the notion that the N-terminal region makes a major contribution to the variation in pB decay rate in the PYP family. Instead, the results imply a major role for residues in the PAS core of PYP for causing the large range of pB decay rates in the PYP family of photoreceptors.

The modest effect of point mutations in the N-terminal region of Hhal PYP on pB life time can be understood based on the results reported here: the accelerating effect of the N-terminal region on pB decay proceeds largely through structurally non-specific interactions. Previous work indicated the importance of a CH/π hydrogen bond between the phenyl ring of Phe6 and the alkyl chain of Lys123 for regulating pB decay[75]. However, the F6A mutation slows down pB decay by a factor ~50, much less than the factor ~2,000 found for N-terminally truncated PYPs. The work reported here indicates that largely non-specific charge-charge interactions of a covalently tethered negatively charged N-terminal region are responsible for most of the accelerating effect of the N-terminal region. The conservation of the excess negative charge on the N-terminal region suggests that such interactions are retained throughout the PYP family of photoreceptors.

The relatively weak and non-specific nature of the interactions between the N-terminal region and the PAS core of PYP in the process of accelerating pB decay indicated by the data reported here are in line with a number of published results. First, in the NMR structure of the pG state of PYP the N-terminal region is the least structured[18], and this region has substantially lower protection factors against H/D exchange than the remainder of PYP[79-82]. Secondly, a number of results have provided strong evidence that the pB state is partially unfolded[31-34, 46, 47], and that concomitantly the N-terminal region is released from the remainder of PYP[8, 36, 37]. Conceptually, a mechanism based on relatively non-specific interactions between the N-terminal region and the PAS core of PYP appears to match the partially unfolded nature of the pB photocycle intermediate.

CHAPTER IV

CONCLUSIONS AND SUGGESTIONS FOR FUTURE WORK

4.1 Summary

A large number of proteins contain small conserved domains (~100 residues), which share a common structural fold, but are highly diverse in both amino acid sequence and functional property. These form large protein superfamilies based on their three-dimensional structural fold. In many of these a linker region joins such conserved domains to other conserved domains in the same protein. Recent evidence suggests that these linker regions play an important role in the functioning of the protein by signal relay between such domains, yet for many the mechanism by which such linkers act is not known. Here we study the functional role of the N-terminal region of the blue light bacterial photoreceptor Photoactive Yellow Protein (PYP), a prototype of the PAS domain superfamily.

An emerging feature from studies on PAS domain protein signaling is the functional importance of N-terminal or C-terminal α-helical extensions. Functionally important conformational changes are known to occur in these extensions, including stimulus-induced release and partial unfolding of the helical region from the PAS core.

In PYP, the N-terminal 25 residues contain two α-helices that pack against the β-sheet in the PAS core. Photoexcitation with blue light converts the pG dark state of PYP into the long-lived pB intermediate state. This is characterized by a blue shift in the absorbance spectrum (446 nm to 355 nm) of the *p*CA, and results in the partial unfolding of the α-helices and release of the N-terminus from the PAS core. In full-length PYP the decay of this pB intermediate back to pG ground state occurs in ~0.4 s. However, deletion of the N-terminal 25-residue helical extension in Δ25 PYP slows the pB decay rate by a factor of ~1,850. In this work we have examined the mechanism by which the N-terminal helical extension of PYP accelerates the pB signaling state of PYP.

Addition of the synthetic 25-residue N-terminal peptide to Δ25 PYP only modestly accelerated the pB decay rate by a factor of ~4; 740 s for Δ25 PYP pB decay and 184 s for Δ25 PYP with the addition of 15 mM N-terminal peptide. We have developed a kinetic model to fit the experimental data that shows the affinity of the peptide for the Δ25 PYP pB state is low (K_d ~10 mM), and when extrapolated to infinite peptide concentration yields a pB lifetime of 121 s. This slight acceleration in pB decay rate due to the addition of the N-terminal peptide is still a factor ~300 less than what is observed in full-length PYP. To better understand this peptide effect on Δ25 PYP, we examined the role of secondary structure in the peptide. Circular dichroism spectroscopy showed the N-terminal peptide to be largely unstructured; therefore we attempted to increase helical content in the peptide by using structure-inducing agents such as trifluoroethanol, ammonium sulfate, and various other kosmotropes. In these experiments we observed that the pB lifetime for Δ25 PYP in the absence of peptide followed a Hofmeister effect, in which kosmotropes accelerated pB decay rate, but only for the

negative ions. We also found that these agents increase the effectiveness of the peptide effect on the pB decay rate of Δ25 PYP, but this increase is relatively small. These results suggest that the changes in helical content caused by the structuring agents only have a minor influence on the magnitude of the peptide effect. This finding implies that the low amount of secondary structure in the peptide has only a small effect on acceleration of the pB decay rate of Δ25 PYP by the N-terminal peptide.

Since the addition of the N-terminal peptide produced only a small acceleration in the pB decay rate of Δ25 PYP, and the addition of structure-inducing agents only modestly increased this peptide effect, we considered how covalent tethering of the N-terminal peptide as seen in full-length PYP might accelerate pB decay. In full-length PYP tethering will result in a high local concentration of the N-terminal peptide that the remaining PAS region of PYP experiences in the full-length protein.

In the next set of experiments we consecutively deleted amino acid residues in the N-terminus of full-length PYP to identify residues of the tethered peptide that play an important role in accelerating pB decay. Consecutive deletion of residues (without His-affinity tag) resulted in a progressive increase in pB lifetime from 1.3 s for Δ4 PYP to 860 s for Δ23 PYP, resulting in ~2,100-fold total increase in pB lifetime. In this deletion mutant series the effect of deletion of each α-helical region can be seen. For deletion mutants in which the His-affinity tag was not removed, the progressive increase in pB lifetime was smaller and more gradual, slowing down from 0.7 s in full-length PYP to 63 s in Δ26 PYP, resulting in only 90-fold total increase in pB lifetime. These results reveal that the presence of the His-affinity tag on the deletion mutants accelerates the pB decay rate in the range of Δ10 PYP through Δ25 PYP, with this accelerating effect becoming

more pronounced in the progressive deletion series. Below Δ10 PYP the affinity tag has little effect on pB decay rate, and in full-length PYP the presence of a His-tag actually slows pB decay. Interestingly, we found that the presence of this 14-residue His-affinity tag on Δ25 PYP accelerated pB decay more effectively than native Δ11 PYP. These both have 11 residues deleted. This implies that the acceleration of pB decay rate by the attachment of N-terminal peptide to Δ25 PYP exhibits a remarkably low level of amino acid sequence conservation, and reiterates the poor affinity of the N-terminal peptide for Δ25 PYP. These observations suggested that the affinity tag contains a sequence feature that accelerates pB decay regardless of the its exact location in the N-terminal region. Further analysis of the affinity tag led us to believe a region of four negative aspartic acid residues (DDDD) was the feature that accelerates pB decay rate. We therefore explored the possibility that the accelerating effect of the N-terminal peptide on pB decay is pH-dependent.

First, we determined the pH dependence of pB decay in Δ25 PYP. This proved to be opposite of that for full-length PYP. For full-length PYP the rate of pB decay is fastest near pH 8 and is slowed down at both lower and higher pH. However, for Δ25 PYP pB decay is slowest near pH 7. Addition of 1 mM N-terminal peptide to Δ25 PYP revealed that the peptide effect on pB decay kinetics is strongly pH dependent, with the accelerating effect largest at pH 5.5 and decreasing to almost no acceleration at pH 4 and pH 9. This pH dependence implies that electrostatic interactions between the N-terminal peptide and the PAS core play a critical role in accelerating the pB decay rate. Therefore, we examined the role of the overall charge in the peptide effect of accelerating pB decay. To do this, we calculated the pH dependence of the net charge of both the N-terminal

peptide and the PAS core of PYP based on their respective amino acid sequences. These calculations showed that the peptide effect on acceleration of pB decay for Δ25 PYP between pH 4 and pH 7 is a result of electrostatic interactions between a positive PAS core and a negative N-terminal peptide. This also provides an explanation for the acceleration in pB decay rate by the affinity tag which contains four consecutive aspartate residues. In the N-terminal deletion mutants the progressive deletion of negatively charged residues in the N-terminus appears to correlate with the resulting deceleration in pB decay rate.

To further understand the structural basis of the electrostatic interactions between the N-terminus and PAS core, we examined the distribution of charged residues found at the molecular surface formed between these two regions in PYP. For this we used the PYP crystal structure (PDB ID 2ZOH). This crystal structure shows several residues (K106, K110, K123), and potentially a histidine residue (H108), in the β-sheet that have positively charged side chains pointed towards the N-terminal region. The position and orientation of these charged residues suggest they may form electrostatic interactions with the negatively charged N-terminal region of PYP.

We wondered if this electrostatic interaction between a positively charge PAS core and a negatively charged N-terminus is a common theme among other members of the PYP family. To address this question, we selected representative PYPs across the phylogenetic tree of the PYP family and calculated the isoelectric points (pI) of both the PAS core and N-terminal regions of each member. In these representative PYPs a distinct pattern is observed for both the PAS core and N-terminus. The average calculated pI for all PAS core regions is 8.36 and the average pI for the N-terminal regions is 4.06. This

clearly shows that for a majority of PYPs the N-terminal region is more negatively charged while the PAS core is more positively charged near neutral pH. Thus, the attractive interaction of a negatively charge N-terminus with a positively charge PAS core appears to be a conserved feature in the PYP family. These electrostatic interactions seem to play an important role in the acceleration of the pB decay rate of PYP.

4.2 Suggestions for future work

Based on this work it appears that electrostatic interactions between the negatively charge N-terminus and positively charged PAS core are a major contributing factor in the acceleration of the pB decay rate in PYP. To better understand which interactions are more important, each negatively charged residue in the N-terminal region or each positively charged residue in the PAS core that is oriented toward the N-terminus could be mutated to a neutral amino acid such as alanine. This would remove the electrostatic interaction at that position and would be expected to slow down the pB decay rate of PYP.

In this work we determined that the N-terminal peptide has low affinity for binding to Δ25 PYP. In order to increase the productive interaction between these a disulfide bridge could be introduced between Δ25 PYP and a synthetic peptide corresponding to the N-terminal region of PYP. One or more cysteine residues could be introduced into both the N-terminal peptide and in the β-sheet region of the PAS core that interacts with the N-terminus. This would allow the N-terminal peptide to better interact with the PAS core through the formation of a disulfide bond between the Cys residues.

The resulting PYP variant would be expected to exhibit a rate of pB decay similar to wild type PYP.

To determine whether the ~300 fold increase in pB decay rate exhibited by the tethering of the N-terminal peptide to the remainder of PYP is a result of high local peptide concentration felt by the PAS region, or rather, a result of more productive collisions between the peptide and PAS domain, the free (not tethered) N-terminal peptide could be added to full-length PYP. Non-productive binding of the free N-terminal peptide to full-length PYP (in place of the tethered N-terminus) would decrease the rate of pB decay.

REFERENCES

1. Orengo, C. A., and Thornton, J. M. (2005) Protein families and their evolution - A structural perspective, In *Annu. Rev. Biochem.*, pp 867-900.
2. Punta, M., Coggill, P. C., Eberhardt, R. Y., Mistry, J., Tate, J., Boursnell, C., Pang, N., Forslund, K., Ceric, G., Clements, J., Heger, A., Holm, L., Sonnhammer, E. L. L., Eddy, S. R., Bateman, A., and Finn, R. D. (2012) The Pfam protein families database, *Nuc. Acids Res. 40*, D290-D301.
3. Schultz, J., Milpetz, F., Bork, P., and Ponting, C. P. (1998) SMART, a simple modular architecture research tool: Identification of signaling domains, *Proc. Natl. Acad. Sci. USA 95*, 5857-5864.
4. Moglich, A., Ayers, R. A., and Moffat, K. (2009) Structure and signaling mechanism of Per-ARNT-Sim domains, *Structure 17*, 1282-1294.
5. van Valen, D., Haataja, M., and Phillips, R. (2009) Biochemistry on a leash: the roles of tether length and geometry in signal integration proteins, *Biophys. J. 96*, 1275-1292.
6. Vogel, C., Bashton, M., Kerrison, N. D., Chothia, C., and Teichmann, S. A. (2004) Structure, function and evolution of multidomain proteins, *Curr. Opin. Struct. Biol. 14*, 208-216.

7. Harigai, M., Yasuda, S., Imamoto, Y., Yoshihara, F., Tokunaga, F., and Kataoka, M. (2001) Amino acids in the N-terminal region regulate the photocycle of photoactive yellow protein, *J. Biochem. 130*, 51-56.

8. van der Horst, M. A., van Stokkum, I. H., Crielaard, W., and Hellingwerf, K. J. (2001) The role of the N-terminal domain of photoactive yellow protein in the transient partial unfolding during signalling state formation, *Febs Letters 497*, 26-30.

9. Harper, S. M., Neil, L. C., and Gardner, K. H. (2003) Structural basis of a phototropin light switch, *Science 301*, 1541-1544.

10. Yildiz, O., Doi, M., Yujnovsky, I., Cardone, L., Berndt, A., Hennig, S., Schulze, S., Urbanke, C., Sassone-Corsi, P., and Wolf, E. (2005) Crystal structure and interactions of the PAS repeat region of the Drosophila clock protein PERIOD, *Mol. Cell 17*, 69-82.

11. Zoltowski, B. D., Schwerdtfeger, C., Widom, J., Loros, J. J., Bilwes, A. M., Dunlap, J. C., and Crane, B. R. (2007) Conformational switching in the fungal light sensor vivid, *Science 316*, 1054-1057.

12. Taylor, B. L., and Zhulin, I. B. (1999) PAS domains: Internal sensors of oxygen, redox potential, and light, *Microb. Mol. Biol. Reviews 63*, 479-506.

13. Ponting, C. P., and Aravind, L. (1997) PAS: a multifunctional domain family comes to light, *Curr. Biol. 7*, R674-R677.

14. Meyer, T. E. (1985) Isolation and characterization of soluble cytochromes, ferredoxins and other chromophoric proteins from the halophilic phototrophic bacterium Ectothiorhodospira halophila, *Biochim. Biophys. Acta 806*, 175-183.

15. Raymond, J. C., and Sistrom, W. R. (1967) The isolation and preliminary characterization of a halophilic photosynthetic bacterium, *Archiv fur Mikrobiologie 59*, 255-268.

16. Raymond, J. C., and Sistrom, W. R. (1969) ctothiorhodospira halophila: a new species ofthe genus Ectothiorhodospira, *Archiv fur Mikrobiologie 69*, 121-126.

17. Singh, K. S., Kirksey, J., Hoff, W. D., and Deole, R. (2014) Draft Genome Sequence of the Extremely Halophilic Phototrophic Purple Sulfur Bacterium Halorhodospira halochloris, *J. Genomics 2*, 118-120.

18. Dux, P., Rubinstenn, G., Vuister, G. W., Boelens, R., Mulder, F. A. A., Hard, K., Hoff, W. D., Kroon, A. R., Crielaard, W., Hellingwerf, K. J., and Kaptein, R. (1998) Solution structure and backbone dynamics of the photoactive yellow protein, *Biochemistry 37*, 12689-12699.

19. van Beeumen, J. J., Devreese, B. V., Vanbun, S. M., Hoff, W. D., Hellingwerf, K. J., Meyer, T. E., McRee, D. E., and Cusanovich, M. A. (1993) The primary structure of a photoactive yellow protein from the phototrophic bacterium, Ectothiorhodospira halophila, with evidence for the mass and the binding site of the chromophore, *Protein Science 2*, 1114-1125.

20. McRee, D. E., Tainer, J. A., Meyer, T. E., Van Beeumen, J., Cusanovich, M. A., and Getzoff, E. D. (1989) Crystallographic structure of a photoreceptor protein at 2.4 A resolution, *Proc Natl Acad Sci U S A 86*, 6533-6537.

21. Hoff, W. D., Dux, P., Hard, K., Devreese, B., Nugterenroodzant, I. M., Crielaard, W., Boelens, R., Kaptein, R., Vanbeeumen, J., and Hellingwerf, K. J. (1994)

Thiol ester-linked p-coumaric acid as a new photoactive prosthetic group in a protein with rhodopsin-like photochemistry, *Biochemistry 33*, 13959-13962.

22. Baca, M., Borgstahl, G. E. O., Boissinot, M., Burke, P. M., Williams, D. R., Slater, K. A., and Getzoff, E. D. (1994) Complete chemical structure of photoactive yellow protein: Novel thioester-linked 4-hydroxycinnamyl chromophore and photocycle chemistry, *Biochemistry 33*, 14369-14377.

23. Kort, R., Hoff, W. D., Van West, M., Kroon, A. R., Hoffer, S. M., Vlieg, K. H., Crielaand, W., Van Beeumen, J. J., and Hellingwerf, K. J. (1996) The xanthopsins: a new family of eubacterial blue-light photoreceptors, *EMBO J 15*, 3209-3218.

24. Borgstahl, G. E. O., Williams, D. R., and Getzoff, E. D. (1995) 1.4 Å structure of photoactive yellow protein, a cytosolic photoreceptor: unusual fold, active site and chromophore, *Biochemistry 34*, 6278-6287.

25. van Aalten, D. M., Crielaard, W., Hellingwerf, K. J., and Joshua-Tor, L. (2000) Conformational substates in different crystal forms of the photoactive yellow protein--correlation with theoretical and experimental flexibility, *Prot. Sci. 9*, 64-72.

26. Hefti, M. H., Francoijs, K. J., de Vries, S. C., Dixon, R., and Vervoort, J. (2004) The PAS fold - A redefinition of the PAS domain based upon structural prediction, *Eu. J. of Biochem. 271*, 1198-1208.

27. Pellequer, J. L., Wager-Smith, K. A., Kay, S. A., and Getzoff, E. D. (1998) Photoactive yellow protein: A structural prototype for the three-dimensional fold of the PAS domain superfamily, *Proc. Natl. Acad. Sci. USA 95*, 5884-5890.

28. Meyer, T. E. (1985) Isolation and characterization of soluble cytochromes, ferredoxins and other chromophoric proteins from the halophilic phototrophic bacterium Ectothiorhodospira halophila, *Biochim. Biophys. Acta 806*, 175-183.

29. Kort, R., Vonk, H., Xu, X., Hoff, W. D., Crielaard, W., and Hellingwerf, K. J. (1996) Evidence for trans-cis isomerization of the p-coumaric acid chromophore as the photochemical basis of the photocycle of photoactive yellow protein, *Febs Letters 382*, 73-78.

30. Bernard, C., Houben, K., Derix, N. M., Marks, D., van der Horst, M. A., Hellingwerf, K. J., Boelens, R., Kaptein, R., and van Nuland, N. A. (2005) The solution structure of a transient photoreceptor intermediate: Delta25 photoactive yellow protein, *Structure 13*, 953-962.

31. Lee, B. C., Croonquist, P. A., Sosnick, T. R., and Hoff, W. D. (2001) PAS domain receptor photoactive yellow protein is converted to a molten globule state upon activation, *J. Biol. Chem. 276*, 20821-20823.

32. Lee, B. C., Pandit, A., Croonquist, P. A., and Hoff, W. D. (2001) Folding and signaling share the same pathway in a photoreceptor, *Proc. Natl. Acad. Sci. USA 98*, 9062-9067.

33. Hoff, W. D., Xie, A., Van Stokkum, I. H. M., Tang, X. J., Gural, J., Kroon, A. R., and Hellingwerf, K. J. (1999) Global conformational changes upon receptor stimulation in photoactive yellow protein, *Biochemistry 38*, 1009-1017.

34. van Brederode, M. E., Hoff, W. D., VanStokkum, I. H. M., Groot, M. L., and Hellingwerf, K. J. (1996) Protein folding thermodynamics applied to the photocycle of the photoactive yellow protein, *Biophys. J. 71*, 365-380.

35. Zhao, J. M., Lee, H., Nome, R. A., Majid, S., Scherer, N. F., and Hoff, W. D. (2006) Single-molecule detection of structural changes during Per-Arnt-Sim (PAS) domain activation, *Proc. Natl. Acad. Sci. U S A 103*, 11561-11566.

36. Imamoto, Y., Kamikubo, H., Harigai, M., Shimizu, N., and Kataoka, M. (2002) Light-induced global conformational change of photoactive yellow protein in solution, *Biochemistry 41*, 13595-13601.

37. Harigai, M., Imamoto, Y., Kamikubo, H., Yamazaki, Y., and Kataoka, M. (2003) Role of an N-terminal loop in the secondary structural change of photoactive yellow protein, *Biochemistry 42*, 13893-13900.

38. Vreede, J., van der Horst, M. A., Hellingwerf, K. J., Crielaard, W., and van Aalten, D. M. F. (2003) PAS domains - Common structure and common flexibility, *J. Biol. Chem. 278*, 18434-18439.

39. Kyndt, J. A., Meyer, T. E., Olson, K. T., Van Beeumen, J., and Cusanovich, M. A. (2013) Photokinetic, Biochemical and Structural Features of Chimeric Photoactive Yellow Protein Constructs, *Photochemistry and Photobiology 89*, 349-360.

40. Meyer, T. E., Yakali, E., Cusanovich, M. A., and Tollin, G. (1987) Properties of a water-soluble, yellow protein isolated from a halophilic phototrophic bacterium that has photochemical activity analogous to sensory rhodopsin, *Biochemistry 26*, 418-423.

41. Sprenger, W. W., Hoff, W. D., Armitage, J. P., and Hellingwerf, K. J. (1993) The Eubacterium Ectothiorhodospira halophila is negatively phototactic, with a

wavelength dependence that fits the absorption spectrum of the photoactive yellow protein, *J. Bacter. 175*, 3096-3104.

42. Cusanovich, M. A., and Meyer, T. E. (2003) Photoactive yellow protein: A prototypic PAS domain sensory protein and development of a common signaling mechanism, *Biochemistry 42*, 4759-4770.

43. Getzoff, E. D., Gutwin, K. N., and Genick, U. K. (2003) Anticipatory active-site motions and chromophore distortion prime photoreceptor PYP for light activation, *Nat. Struct. Biol. 10*, 663-668.

44. Hellingwerf, K. J., Hendriks, J., and Gensch, T. (2003) Photoactive Yellow Protein, a new type of photoreceptor protein: Will this "yellow lab" bring us where we want to go?, *J. Phys. Chem. A 107*, 1082-1094.

45. Hoff, W. D., Vanstokkum, I. H. M., Vanramesdonk, H. J., Vanbrederode, M. E., Brouwer, A. M., Fitch, J. C., Meyer, T. E., Vangrondelle, R., and Hellingwerf, K. J. (1994) Measurement and global analysis of the absorbance changes in the photocycle of the photoactive yellow protein from Ectothiorhodospira halophila, *Biophys. J. 67*, 1691-1705.

46. Bernard, C., Houben, K., Derix, N. M., Marks, D., van der Horst, M. A., Hellingwerf, K. J., Boelens, R., Kaptein, R., and van Nuland, N. A. J. (2005) The solution structure of a transient photoreceptor intermediate: Delta 25 photoactive yellow protein, *Structure 13*, 953-962.

47. Zhao, J. M., Lee, H., Nome, R. A., Majid, S., Scherert, N. F., and Hoff, W. D. (2006) Single-molecule detection of structural changes during Per-Arnt-Sim (PAS) domain activation, *Proc. Natl. Acad. Sci. USA 103*, 11561-11566.

48. Moglich, A., Ayers, R. A., and Moffat, K. (2009) Design and Signaling Mechanism of Light-Regulated Histidine Kinases, *J. Mol. Biol. 385*, 1433-1444.

49. Louis-Jeune, C., Andrade-Navarro, M. A., and Perez-Iratxeta, C. (2012) Prediction of protein secondary structure from circular dichroism using theoretically derived spectra, *Proteins 80*, 374-381.

50. Jian, X. Y., Clark, W. A., Kowalak, J., Markey, S. P., Simonds, W. F., and Northup, J. K. (2001) GB gamma affinity for bovine rhodopsin is determined by the carboxyl-terminal sequences of the gamma subunit, *J. Biol. Chem. 276*, 48518-48525.

51. Sourjik, V., and Berg, H. C. (2002) Binding of the *Escherichia coli* response regulator CheY to its target measured in vivo by fluorescence resonance energy transfer, *Proc. Natl. Acad. Sci. USA 99*, 12669-12674.

52. Luo, P. Z., and Baldwin, R. L. (1997) Mechanism of helix induction by trifluoroethanol: A framework for extrapolating the helix-forming properties of peptides from trifluoroethanol/water mixtures back to water, *Biochemistry 36*, 8413-8421.

53. Khoroshyy, P., Der, A., and Zimanyi, L. (2011) Kinetic effect of Hofmeister ions on the photocycle of photoactive yellow protein, *Eur. Biophys. J. Biophys. Lett. 40*, 208-208.

54. Khoroshyy, P., Der, A., and Zimanyi, L. (2013) Effect of Hofmeister cosolutes on the photocycle of photoactive yellow protein at moderately alkaline pH, *J. Photochem. and Photobiol. B-Biol. 120*, 111-119.

55. Timpe, L. C., and Peller, L. (1995) A random flight chain model for the tether of the shaker K+ channel inactivation domain, *Biophys. J. 69*, 2415-2418.

56. Windisch, B., Bray, D., and Duke, T. (2006) Balls and chains - A mesoscopic approach to tethered protein domains, *Biophys. J. 91*, 2383-2392.

57. Yao, X. L., Rosen, M. K., and Gardner, K. H. (2008) Estimation of the available free energy in a LOV2-J alpha photoswitch, *Nat. Chem. Biol. 4*, 491-497.

58. Elove, G. A., Bhuyan, A. K., and Roder, H. (1994) Kinetic mechanisms of cytochrome c folding. Involvement of the heme and its ligands., *Biochemistry 33*, 6925-6935.

59. Kiefhaber, T. (1995) Kinetic traps in lysozyme folding, *Proc. Natl. Acad. Sci. USA 92*, 9029-9033.

60. Hoff, W. D., Van Stokkum, I. H. M., Gural, J., and Hellingwerf, K. J. (1997) Comparison of acid denaturation and light activation in the eubacterial blue-light receptor photoactive yellow protein, *Biochim. Biophys. Acta 1322*, 151-162.

61. Genick, U. K., Devanathan, S., Meyer, T. E., Canestrelli, I. L., Williams, E., Cusanovich, M. A., Tollin, G., and Getzoff, E. D. (1997) Active site mutants implicate key residues for control of color and light cycle kinetics of photoactive yellow protein, *Biochemistry 36*, 8-14.

62. Bjellqvist, B., Hughes, G. J., Pasquali, C., Paquet, N., Ravier, F., Sanchez, J. C., Frutiger, S., and Hochstrasser, D. (1993) The focusing positions of polypeptides in immobilized pH gradients can be predicted from their amino acid sequences, *Electrophoresis 14*, 1023-1031.

63. McRee, D. E., Meyer, T. E., Cusanovich, M. A., Parge, H. E., and Getzoff, E. D. (1986) Crystallographic characterization of a photoactive yellow protein with photochemistry similar to rhodopsin, *J. Biol. Chem. 261*, 3850-3851.

64. Kumauchi, M., Hara, M. T., Stalcup, P., Xie, A. H., and Hoff, W. D. (2008) Identification of six new photoactive yellow proteins - Diversity and structure-function relationships in a bacterial blue light photoreceptor, *Photochem. Photobiol. 84*, 956-969.

65. Meyer, T. E., Kyndt, J. A., Memmi, S., Moser, T., Colon-Acevedo, B., Devreese, B., and Van Beeumen, J. J. (2012) The growing family of photoactive yellow proteins and their presumed functional roles, *Photochem. Photobiol. Sci. 11*, 1495-1514.

66. Hospes, M., Ippel, J. H., Boelens, R., Hellingwerf, K. J., and Hendriks, J. (2012) Binding of Hydrogen-Citrate to Photoactive Yellow Protein Is Affected by the Structural Changes Related to Signaling State Formation, *J. Phys. Chem. B 116*, 13172-13182.

67. Shimizu, N., Imamoto, Y., Harigai, M., Kamikubo, H., Yamazaki, Y., and Kataoka, M. (2006) pH-dependent equilibrium between long lived near-UV intermediates of photoactive yellow protein, *J. Biol. Chem. 281*, 4318-4325.

68. Shimizu, N., Kamikubo, H., Mihara, K., Imamoto, Y., and Kataoka, M. (2002) Effect of organic anions on the photoreaction of photoactive yellow protein, *J. Biochem. 132*, 257-263.

69. Zhang, Y. J., and Cremer, P. S. (2006) Interactions between macromolecules and ions: the Hofmeister series, *Curr. Opin. Chem. Biol. 10*, 658-663.

70. Memmi, S., Kyndt, J., Meyer, T., Devreese, B., Cusanovich, M., and Van Beeumen, J. (2008) Photoactive yellow protein from the halophilic bacterium Salinibacter ruber, *Biochemistry 47*, 2014-2024.

71. Haker, A., Hendriks, J., van Stokkum, I. H. M., Heberle, J., Hellingwerf, K. J., Crielaard, W., and Gensch, T. (2003) The two photocycles of photoactive yellow protein from Rhodobacter sphaeroides, *J. Biol. Chem. 278*, 8442-8451.

72. Kyndt, J. A., Hurley, J. K., Devreese, B., Meyer, T. E., Cusanovich, M. A., Tollin, G., and Van Beeumen, J. J. (2004) Rhodobacter capsulatus photoactive yellow protein: genetic context, spectral and kinetics characterization, and mutagenesis, *Biochemistry 43*, 1809-1820.

73. Kumauchi, M., Kaledhonkar, S., Philip, A. F., Wycoff, J., Hara, M., Li, Y. X., Xie, A. H., and Hoff, W. D. (2010) A conserved helical capping hydrogen bond in PAS domains controls signaling kinetics in the superfamily prototype photoactive yellow protein, *J. Am. Chem. Soc. 132*, 15820-15830.

74. Philip, A. F., Kumauchi, M., and Hoff, W. D. (2010) Robustness and evolvability in the functional anatomy of a PER-ARNT-SIM (PAS) domain, *Proc. Natl. Acad. Sci. USA 107*, 17986-17991.

75. Harigai, M., Kataoka, M., and Imamoto, Y. (2006) A single CH/pi weak hydrogen bond governs stability and the photocycle of the photoactive yellow protein, *J. Am. Chem. Soc. 128*, 10646-10647.

76. Devanathan, S., Genick, U. K., Canestrelli, I. L., Meyer, T. E., Cusanovich, M. A., Getzoff, E. D., and Tollin, G. (1998) New insights into the photocycle of Ectothiorhodospira halophila photoactive yellow protein: photorecovery of the

long-lived photobleached intermediate in the Met100Ala mutant, *Biochemistry 37*, 11563-11568.

77. Kumauchi, M., Hamada, N., Sasaki, J., and Tokunaga, F. (2002) A role of methionine100 in facilitating PYPM-decay process in the photocycle of photoactive yellow protein, *J. Biochem. 132*, 205-210.

78. Morishita, T., Harigai, M., Yamazaki, Y., Kamikubo, H., Kataoka, M., and Imamoto, Y. (2007) Array of aromatic amino acid side chains located near the chromophore of photoactive yellow protein, *Photochem. Photobiol. 83*, 280-285.

79. Brudler, R., Gessner, C. R., Li, S., Tyndall, S., Getzoff, E. D., and Woods, V. L. (2006) PAS domain allostery and light-induced conformational changes in photoactive yellow protein upon I-2 intermediate formation, probed with enhanced hydrogen/deuterium exchange mass spectrometry, *J. Mol. Biol. 363*, 148-160.

80. Cheng, G. L., Cusanovich, M. A., and Wysocki, V. H. (2006) Properties of the dark and signaling states of photoactive yellow protein probed by solution phase hydrogen/deuterium exchange and mass spectrometry, *Biochemistry 45*, 11744-11751.

81. Craven, C. J., Derix, N. M., Hendriks, J., Boelens, R., Hellingwerf, K. J., and Kaptein, R. (2000) Probing the nature of the blue-shifted intermediate of photoactive yellow protein in solation by NMR: Hydrogen-deuterium exchange data and pH studies, *Biochemistry 39*, 14392-14399.

82. Rubinstenn, G., Vuister, G. W., Mulder, F. A. A., Dux, P. E., Boelens, R., Hellingwerf, K. J., and Kaptein, R. (1998) Structural and dynamic changes of

photoactive yellow protein during its photocycle in solution, *Nature Struct. Biol. 5*, 568-570.

VITA

DANNY L. MAPLES

Candidate for the Degree of

Doctor of Philosophy

Thesis: FUNCTIONAL STUDIES ON THE N-TERMINAL REGION OF PHOTOACTIVE YELLOW PROTEIN

Major Field: CHEMISTRY

Biographical:

Education:

Completed the requirements for the Doctor of Philosophy in Chemistry at Oklahoma State University, Stillwater, Oklahoma in July 2015.

Completed the requirements for the Bachelor of Arts in Chemistry at Southwestern Oklahoma State University, Weatherford, OK/USA in 2006.

Experience: Teaching and Research Assistant in the Department of Chemistry, Oklahoma State University, Stillwater, OK.